Journal of Hydrology 555 (2017) 489–505

Contents lists available at ScienceDirect

Journal of Hydrology

journal homepage: www.elsevier.com/locate/jhydrol

Research papers

Remote sensing upscaling of interception loss from isolated oaks: Sardon catchment case study, Spain

S.M. Tanvir Hassan [a,b], Chandra Prasad Ghimire [a], Maciek W. Lubczynski [a,*]

[a] Department of Water Resources, Faculty of Geo-Information Science and Earth Observation (ITC), University of Twente, PO Box 217, 7500 AE Enschede, The Netherlands
[b] Bangladesh Centre for Advanced Studies (BCAS), Road 16a, House 10, Gulshan, Dhaka 1212, Bangladesh

ARTICLE INFO

Article history:
Received 20 September 2016
Received in revised form 11 May 2017
Accepted 10 August 2017
Available online 17 August 2017
This manuscript was handled by K. Georgakakos, Editor-in-Chief, with the assistance of Xin Li, Associate Editor

Keywords:
Mediterranean oak-woodland catchment
Tree interception loss measurements
Revised Gash's analytical interception loss model
Remote sensing upscaling
Spatio-temporal interception loss mapping

ABSTRACT

Tree interception loss from two Mediterranean oak species, *Quercus ilex* (*Q.i.*) and *Quercus pyrenaica* (*Q.p.*), was estimated during 2-year period (1 October 2011 to 30 September 2013) in sparsely vegetated Sardon catchment (~80 km^2, Spain) by: i) rainfall, throughfall and stemflow measurements; ii) Gash model temporal extrapolation; and iii) remote-sensing spatial upscaling. The annual, measured tree interception losses (I_m) of *Q.i.* and *Q.p.* in the first year were 51% and 16% of *P* (335 mm) and in the second, 46% and 10% of *P* (672 mm), respectively. The revised Gash analytical model of rainfall interception loss, extrapolated well the I_m temporal variability of *Q.i.* and *Q.p.*, provided the throughfall-based, and not Pennman-Monteith-based, average wet canopy evaporation rates were used. Finally, a novel method of spatial upscaling of a tree-based interception loss into plot- and catchment-scale, using per-species, reference tree interception loss and object-attributes derived from satellite imagery, was proposed. The interception losses from *Q.i.* and *Q.p.* were upscaled first into two homogeneous plots (1-ha each and both with ~20% canopy cover), one with *Q.i.* and the other with *Q.p.* oaks and then into the entire Sardon catchment with ~7% canopy cover. The obtained annual-mean, plot interception losses were 9.5% of *P* in evergreen *Q.i.* and 2.5% of *P* in deciduous *Q.p.* plot. The annual-mean catchment interception loss was 1.4% of *P*. The proposed upscaling method is expected to improve catchment water balances, replacing common arbitrary or literature based tree interception loss estimates.

1. Introduction

Rainfall interception losses by forest canopies are usually substantial and sometimes, even a dominant fraction of evapotranspiration (e.g., Gärdenäs and Jansson, 1995; Ghimire et al., 2014; Hörmann et al., 1996; Schellekens et al., 1999; Tiktak and Bouten, 1994). Rainfall interception loss by grasslands or shrub lands is relatively low, <10% of rainfall, but by forests, particularly in temperate climatic environments, is larger and typically accounts for 10–20% for broad-leafed forests and 20–40% for conifer forests (Le Maitre et al., 1999). In arid and semi-arid savannah water limited environments, where trees are sparse and isolated while grasses are dormant throughout most of a year, tree interception loss is largely dependent on tree density and tree canopy cover; besides it is typically lower than in temperate climates, although its relative value in % of rainfall by a single tree is higher than in temperate climates (e.g., David et al., 2006; Mateos and Schnabel, 2001; Pereira et al., 2009a).

Tree interception loss can reduce substantially the amount of water that reaches a ground surface and thereby reduces the available water for aquifer recharge and streamflow, often largely declining water resources. However, unfortunately, it is still a common practice in hydrological catchment modelling to assign tree interception loss either based on selected tree measurements or even arbitrarily (e.g., based on other studies), which can be a source of substantial error. Therefore, experimentally-based, spatial assessment of tree interception loss is an important step in any water balance assessment and modelling.

Rainfall partitioning by tree canopies is a complex process affected by several biotic and abiotic factors (Carlyle-Moses and Gash, 2011; Levia and Frost, 2003; Levia and Frost, 2006). The process of evaporation of intercepted water becomes even more complex where vegetation is sparse as the gaps and ventilation in and between the canopies enhance evaporation rate from the canopy (Teklehaimanot et al., 1991). Moreover, the high variability of rainfall amount and intensity in the Mediterranean climate, adds

* Corresponding author. Tel.: +31 53 4874277; fax: +31 53 4874336.
E-mail address: m.w.lubczynski@utwente.nl (M.W. Lubczynski).

http://dx.doi.org/10.1016/j.jhydrol.2017.08.016
0022-1694/

additional complication to rainfall partitioning by canopy (David et al., 2005; Llorens et al., 2011, 1997).

The interception loss studies conducted so far have largely attempted to quantify the tree interception loss at the single tree or plot level (e.g., David et al., 2006; Gash and Morton, 1978; Ghimire et al., 2012; Mateos and Schnabel, 2001; Pereira et al., 2009a). However, distributed models commonly used in water management and planning, require reliable tree interception loss input in large areas, typically at the catchment-scale (e.g., Henson et al., 2013; Markstrom et al., 2008). To the best of authors' knowledge, none of tree interception loss studies done so far provided such solution at the catchment-scale.

The primary aim of this study, therefore, is to propose an efficient methodology of quantifying the daily tree rainfall interception loss in sparsely vegetated forest, at the catchment-scale. To develop and test that methodology, the Sardon catchment (~80 km^2) in Spanish oak woodland with only two species, *Quercus ilex* (*Q.i.*) and *Quercus pyrenaica* (*Q.p.*) was selected. For the spatial upscaling of tree-based interception loss, direct measurements of rainfall, throughfall and stemflow on both tree species during 2-year period were used, while for temporal extrapolation (or scaling), revised analytical interception loss model (Gash et al., 1995) was applied. The tree interception loss measurements were upscaled to the catchment-scale using remote sensing tree object-attributes, derived from the high resolution satellite imagery, while the calibrated model result was used to reconstruct 3-year, daily tree interception loss in the Sardon catchment. Finally, the implications of the upscaled tree interception loss, e.g., for the spatio-temporal catchment water balance, are discussed briefly.

2. Study area

The Sardon catchment (~80 km^2) is located in central-western Spain about 40 km, west of Salamanca (Fig. 1). It has a hilly landscape and is mainly composed of weathered and fractured granites. The dominant pasture lands in the study area are characterized by natural woody-shrub vegetation of an oak savannah type. The altitude varies from 860 m above the sea level (a.s.l.), at the southern catchment boundary to 733 m a.s.l. at the Sardon river outlet at the northern boundary. There are two types of tree species in the study area, evergreen holm oak *Q.i.* and the broad-leafed deciduous Pyrenean oak *Q.p.*, commonly leafless from December to April. *Q.i.* trees, naturally grow in areas with a dry, Mediterranean climate, over a large range of altitudes from 300 to 1800 m a.s.l. (Terradas, 1999). *Q.p.* is common in the Mediterranean and Euro-Siberian biogeographic regions while in Spain, most of them occur where the summer dry period is less marked, especially in mountainous areas, with altitude ranging from 400 to 1600 m a.s.l., receiving yearly 400–1200 mm of precipitation (Tárrega et al., 2009). The land cover type of the Sardon catchment is typical for the western Pyrenean Peninsula, characterized by sparse oak trees with grasses and patches of evergreen *Cytisus scoparius* shrubs. In Spain, such land cover type is known as *dehesa* and in Portugal as *montado* (Campos et al., 2013).

The climate in the Sardon catchment is semi-arid, typical for the central Iberian Peninsula. The 64-year mean rainfall (October 1950 to September 2014) of the study area is 589 (±177) mm·y^{-1}. Due to the relatively flat topography and location far away from seaside, the spatial variability of rainfall in the study area is small

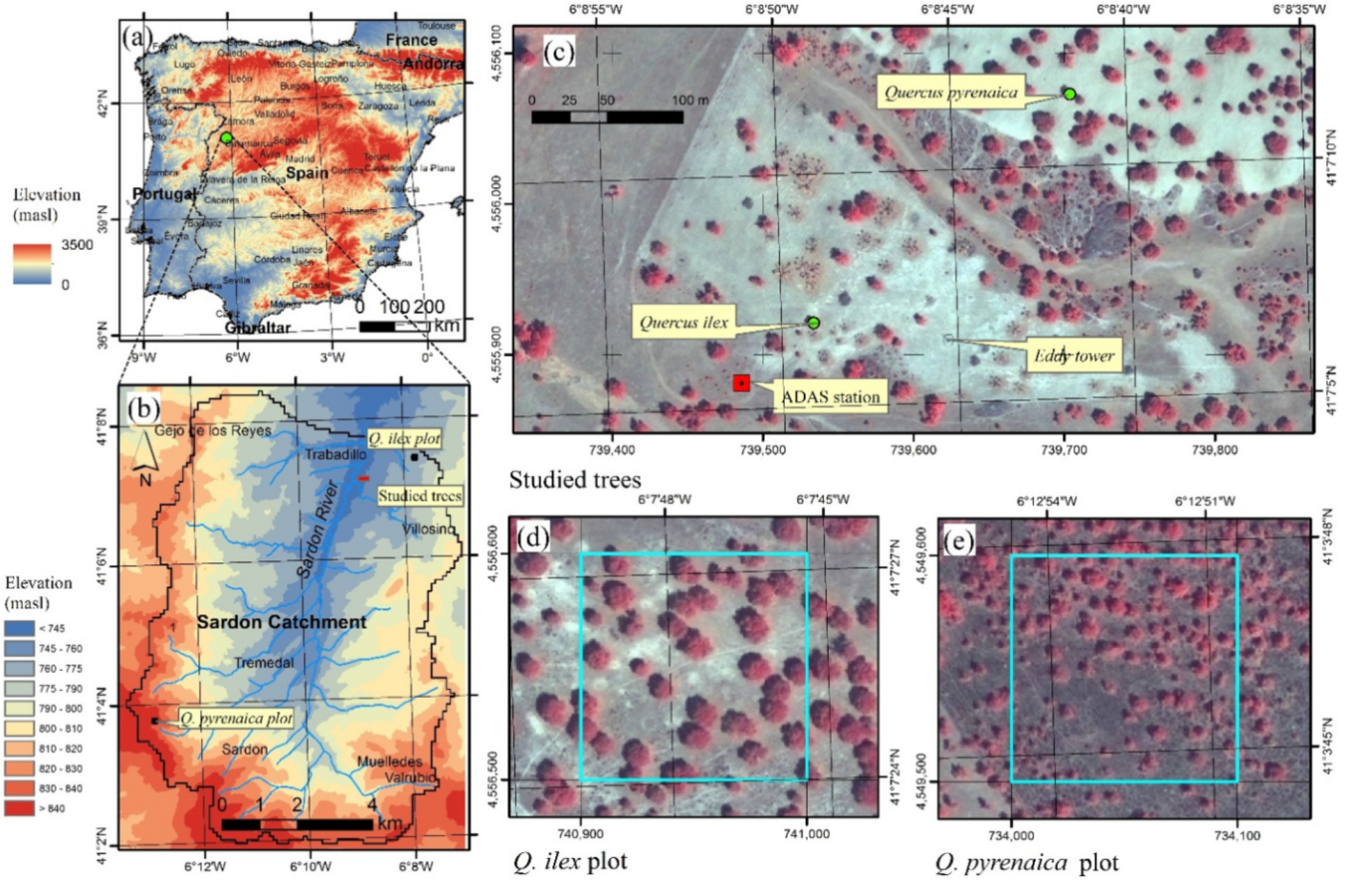

Fig. 1. Study area: a) inset map of Iberian Peninsula; b) Sardon catchment in western Spain; c) location of two studied trees, ADAS station, and eddy covariance tower; d) *Quercus ilex* plot and; e) *Quercus pyrenaica* plot.

(Lubczynski and Gurwin, 2005). The driest and the warmest months are July and August with the mean rainfall of 0.5 (±0.6) mm·d^{-1}, temperature of 21 (±1.5) °C, mean potential evapotranspiration (*PET*) of 5.1 (±0.9) mm·d^{-1}. The wettest months are October to December with rainfall 2.3 (±1.8) mm·d^{-1}, while the coldest are December and January with mean temperature of 5.4 (±1.8) °C and mean *PET* 0.8 (±0.2) mm·d^{-1}.

3. Materials and methods

3.1. Rainfall

Gross rainfall (*P*, mm) was monitored during 2-year period, from 1 October 2011 to 30 September 2013, using a tipping bucket rain gauge (Davis Instruments, USA; 0.2 mm per tip) installed at the automated data acquisition system (ADAS) near Trabadillo (Fig. 1). The orifice of the rain gauge was positioned at 1 m above the ground surface to avoid ground splash effects. The automatically recorded rainfall data were stored by a HOBO event logger (Onset Computer Corporation, USA). The rainfall totals were corrected for the wind speed acquired hourly within the ADAS station together with other micrometeorological data (see below), following the method outlined by Yang et al. (1999).

3.2. Throughfall

Throughfall (*Tf*, mm) in the *Q.i.* and *Q.p.* trees was monitored during 2-year period from 1 October 2011 to 30 September 2013 under one tree per species. *Tf* was measured using tipping buckets (Davis Instruments, USA, 0.2 mm per tip) equipped with HOBO event loggers (Onset Computer Corporation, USA). Under each tree, four tipping bucket devices were installed at 1 m height to avoid ground splash effects and distributed in four directions (Fig. 2), at half-way distance between canopy edges and a stem in order to minimize the effects of spatial variability on the magnitude of average *Tf* (cf. David et al., 2006; Lloyd et al., 1988; Mateos and Schnabel, 2001; Pereira et al., 2009a). The tipping buckets were cleaned once a month to prevent the clogging by organic debris. Regarding the number and locations of the gauges used, it was assumed that four gauges per each tree species, as distributed in this study (Fig. 2), was sufficient to derive reliable mean throughfall per tree, i.e. that the locations of the gauges at half-distance between canopy edge and tree trunk were negligibly affected by angular rainfall (see below). That schema was not as detailed as for example the one proposed by David et al. (2006) due to financial and logistical limitations of this project. However, it will be shown that despite these limitations, this study monitoring schema, with 4-gauges per tree, in the particular Sardon condition, was sufficient to derive reliable mean throughfall per tree.

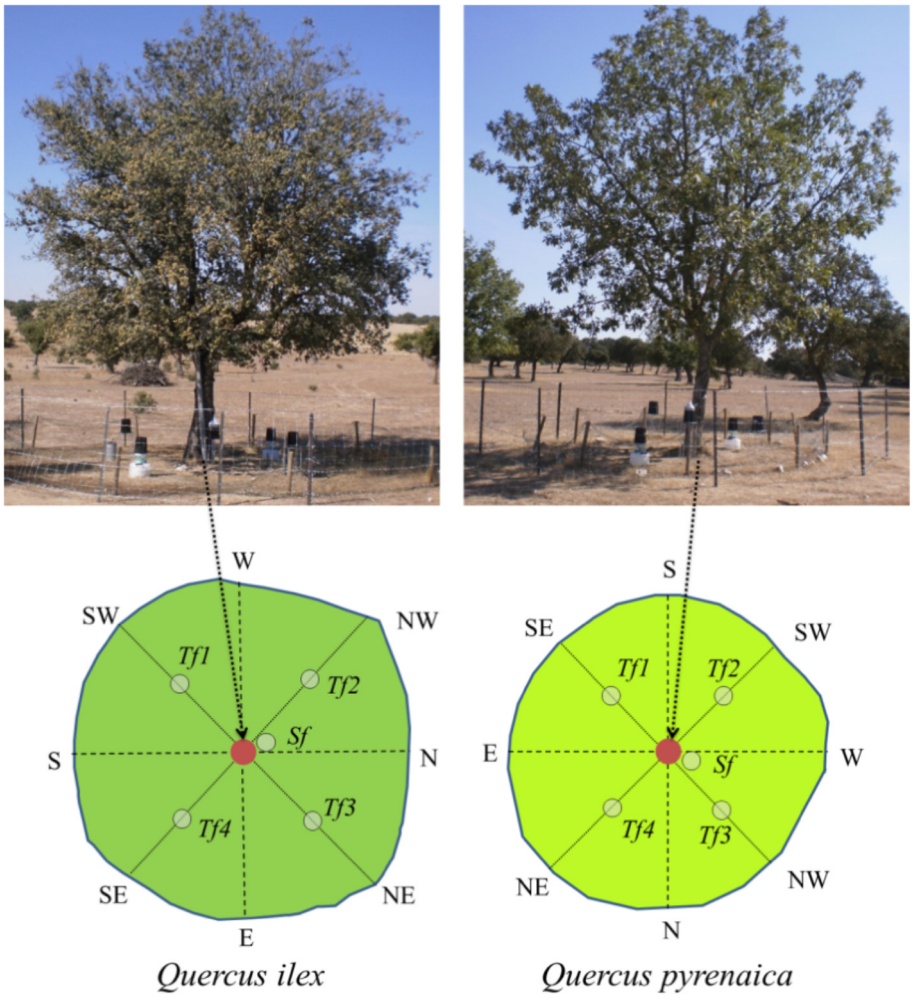

Fig. 2. Photographs and plan view schematics of experimental design for the throughfall and stemflow measurements at the *Quercus ilex* and *Quercus pyrenaica* trees in the Sardon catchment, Spain; *Tf1*, *Tf2*, *Tf3*, and *Tf4* are gauges for throughfall measurements; *Sf* is gauge for stemflow measurement.

3.3. Stemflow

Stemflow (*Sf*, mm) of each tree species was measured during 2-year period, from 1 October 2011 to 30 September 2013, on the same two trees as *Tf* measurements. The *Sf* was measured using tipping buckets (Davis Instruments, USA; 4.3 ml per tip) and was recorded by HOBO event loggers. The tipping buckets were connected to flexible polythene tubing fitted around the circumference of the trunk in a spiral fashion, at 1.5 m from the ground. The orifice of the tipping bucket was covered by a plastic funnel upside down in order to prevent any *Tf* input via orifice. Bark material was removed to provide a clean and smooth surface upon fitting the tube. Any remaining gaps between the stem and polythene tube were sealed using silicon sealant. The recorded stemflow volume was converted to equivalent water depth (mm) by dividing the volume of water by the corresponding tree canopy projection area.

3.4. Rainfall inclination angle and wind direction

Several studies have shown that particularly in sparse tree environments, rainfall inclination angle (RIA) is the important variable to characterize the wind-driven rainfall beneath the canopy (windward and leeward side) (David et al., 2006; King and Harrison, 1998; Xiao et al., 2000b). In order to examine the possible effect of wind-driven rainfall on *Tf* measurement, RIA (in degrees from the vertical) was calculated as described by David et al. (2006). The hourly RIA was computed using hourly rainfall and wind speed data. The average RIA for a rainfall event was calculated as the weighted average of the hourly values, with the weight being the hourly rainfall.

The wind direction (WD) was available in the study area only for the first 2-month (from October 1 till December 3, 2011) of the 2-year study period. That WD data was acquired with Vaisala Multi-Weather Sensor WXT510 at 5-min interval, installed at 10 m height in the eddy covariance tower, located 140 m northeast of the ADAS station (Fig. 1). The daily WD data were also available for the Salamanca station of the Spanish meteorological agency (AEMET). This data were correlated with the 2-month WD data. Finally, both, the WD and RIA were examined whether they have any effect on variability of *Tf*-measurements, i.e., whether there was any wind-driven rainfall input from outside canopy to the *Tf*-gauge measurements beneath the canopy.

3.5. Tree interception loss

The measured tree interception loss per ground-projected canopy area (I_m, mm) was derived as the difference between measured P (mm) and arithmetic mean of four *Tf* (mm) measurements and *Sf* (mm) measurement, for a given tree as follows:

$$I_m = P - Tf - Sf \quad (1)$$

3.6. Additional meteorological measurements

Additional micro-meteorological measurements were acquired through the ADAS station (Fig. 1); these included: net shortwave solar radiation measured using two Kipp & Zonen CMP-3 Pyranometers, soil heat flux with Campbell Scientific's thermocouple sensor at 10 cm depth; relative humidity and air temperature at 2 m height using Eijkelkamp sensors and at 6 m height using Skye sensors, both protected against direct sunlight and precipitation by radiation shields and wind speed also at 2 and 6 m height, using two A100R Vector Instruments (UK) anemometers. All the measurements were acquired by a DL-2e Delta-T Devices (UK) logger applying 5-min interval of data sampling averaged every 1-h.

3.7. Tree characteristics

In addition to 90 *Q.i.* and 84 *Q.p.* trees characterized by Reyes-Acosta and Lubczynski (2013) in the same Sardon study area, tree characteristics were further defined in this study on randomly selected 12 *Q.i.* and 13 *Q.p.* trees. These included tree heights, canopy projection areas, DBH (diameter at breast height) and LAI (leaf area index), the latter because of its positive correlation with tree interception loss at given climatic conditions (Gómez et al., 2001; van Dijk and Bruijnzeel, 2001). The LAI was estimated: i) at single trees, by field measurements conducted on 7–8 September 2010 using a Licor LAI 2000 Plant Canopy Analyzer where more than half of the measurements were repeated for quality purpose; ii) at the catchment scale, at 1-ha grid resolution, through its relation with normalized difference vegetation index (NDVI) (Qi et al., 2000) obtained by image processing of multispectral QuickBird image of 20 August 2009.

3.8. Modelling tree interception loss

Modelling tree interception loss can be used either to fill data gaps or to temporally extrapolate (or scale) tree interception loss forward or backward. In this study, the revised version of analytical rainfall interception loss model (Gash et al., 1995) was used to extrapolate forward and backward, tree interception loss of two tree species *Q.i.* and *Q.p*. To do so, first calibration and validation of the model was performed using 2-year measurements (1st – hydrologic year 2012 assigned as the calibration period and the 2nd – hydrologic year 2013 assigned as the validation period, the two further referred to as HY2012 and HY2013 respectively). Once Gash model parameters were defined, the tree interception losses were extrapolated two years backward (HY2011 and HY2010) and one year forward (HY2014).

Gash et al. (1995) proposed a revision of Gash's (1979) analytical model to estimate interception losses from sparse forests. The revised version of Gash's analytical model takes the sparseness of the canopy into consideration by scaling the mean evaporation rate during a rain event and canopy storage capacity to the proportion of canopy cover where present – for full description see Gash et al. (1995). For a canopy cover of 100% the revised model (Gash et al., 1995) is identical to its basic version (Gash, 1979). The revised Gash model assumes rainfall to occur as a series of discrete events. A discrete rainfall event was defined in this study as an event separated by at least 6 h without rain (to allow drying up the canopy) between two adjacent rainfall events during day time and by at least 12 h at night time as recommended by Mużyło et al. (2012). Each rainfall event of sufficient magnitude was then sub-divided into three phases: a) a wetting-up phase, during which gross rainfall (P) is less than the amount required to fully saturate the canopy (P'); b) a saturation phase, when rainfall intensity (R) exceeds the average evaporation rate from the wet canopy ($\bar{E}$); and c) a drying out phase, after all drips from the canopy have ceased. Table 1

Table 1
Five terms in the revised form of Gash analytical model of interception loss (after Gash et al., 1995).

Component of interception loss	Formulation
1. m small storms insufficient to saturate the canopy ($P < P'$)	$c\sum_{j=1}^{m} P_j$
2. Wetting-up of canopy in n large storms ($P' \geq P$)	$ncP' - ncS_c$
3. Evaporation from the saturated canopy until rainfall and throughfall cease	$c\frac{\bar{E}_c}{\bar{R}}\sum_{j=1}^{n}(P_j - P')$
4. Evaporation after rainfall and throughfall cease	ncS_c
5. Evaporation from trunks; q storms with $P > S_t/p_t$, which saturate the canopy	$qS_t + p_t\sum_{j=1}^{n-q} P_j$

summarizes the equations that are used in the revised Gash's model to calculate the tree interception loss associated with the respective phases. The amount of water needed to saturate completely the canopy (P') is calculated after Gash et al. (1995) from:

$$P' = -\frac{\bar{R}S_c}{\overline{E_c}}\ln\left(1-\frac{\overline{E_c}}{\bar{R}}\right) \quad (2)$$

where $\bar{R}$ denotes the average rainfall intensity falling onto a saturated canopy and S_c, the canopy capacity per unit area of canopy cover, obtained by dividing the canopy storage capacity (S) by the canopy cover fraction (c); similarly the $\bar{E}$ is downscaled in proportion to the canopy cover fraction to obtain the evaporation rate per unit canopy cover ($\overline{E_c}$). Rainfall rates $\geq$0.5 mm·h^{-1} are assumed to represent saturated canopy conditions (Gash, 1979; Schellekens et al., 1999). The free throughfall coefficient (p, here assumed to be equal to $1-c$) is a proportion of rainfall that falls directly on the forest floor without hitting the canopy. Gash (1979) has shown that the slope of a regression equation of measured tree interception loss vs. rainfall should equal to $\bar{E}/\bar{R}$, assuming that both $\bar{E}$ and $\bar{R}$ are constant for all storms. Thus $\bar{E}$ can be estimated from $\bar{R}$ in the absence of above-canopy climatic observations (Bruijnzeel et al., 1987; Dykes, 1997; Holwerda et al., 2012; Schellekens et al., 1999).

The S for the two tree species was estimated using the method of Jackson (1975). In that method, the S is the difference between P and Tf at the inflection point of the P vs. Tf graph. The inflection point is defined as the intersection of the two regressions between P and Tf for the storms that do, and for those that do not fill the canopy storage. The method also allows the derivation of p from the slope of the regression between P and Tf for storms that cannot fill the canopy storage capacity.

The revised version of Gash analytical model was run on an event basis using the respective parameter values derived for each tree. Several calibration runs were done. Once the parameters were derived, the model was run for validation. Finally, the model was run for temporal extrapolation (2-year backward and 1-year forward) using $\bar{E}$ as described in the following paragraph.

The $\bar{E}$ was estimated in two different ways. First, an estimate of $\bar{E}$ was made following the method of Gash (1979), in which $\bar{E}$ was derived from $\bar{E}/\bar{R}$ (i.e., the slope of the linear regression of P against measured tree interception loss), and $\bar{R}$ from the tipping bucket rain gauge record. The value of $\bar{E}$ derived this way is referred to as the Tf-based average wet canopy evaporation rate ($\overline{E_{Tf}}$) and it represents the rate per unit area of canopy projected area, including the gaps within the canopy. Second, the estimate of $\bar{E}$ was made by the Penman-Monteith (P-M) equation, hereafter referred to as $\overline{E_{PM}}$, based on weather data and the canopy resistance (r_s) set to zero (Monteith, 1965) and the aerodynamic resistance (r_a) calculated based on the wind speed and surface roughness characteristics following Thom (1975). The $\overline{E_{PM}}$ derived this way represents the rate per unit area of canopy cover, where the evaporation from the open area (gaps within the canopy in this case) is assumed zero (cf. Valente et al., 1997). The P-M calculation was carried out despite it was expected that the resulting estimate of $\overline{E_{PM}}$ could be underestimated due to the uncertainty of r_a in a sparsely vegetated ecosystem with isolated trees by the Thom (1975) approach (e.g., Pereira et al., 2009b; Teklehaimanot et al., 1991).

3.9. Upscaling tree interception loss into the plot- and catchment-scale

For the spatial upscaling of tree interception loss into plot- and catchment-scale, the classified per species, tree canopy area map delineated by Reyes-Acosta and Lubczynski (2013), was used. The map was derived by combining: (i) a supervised-classification; (ii) an object-oriented classification; and (iii) a comparison of seasonal variation of the leaf status of the two tree species using two high spatial resolution pan-sharpened multi-spectral images, the *QuickBird* image of 0.6 m spatial resolution of 20 August 2009 when both *Q.i.* and *Q.p.* trees were in leafs and the *WorldView-II* image of 0.5 m spatial resolution of 14 December 2010, when *Q.i.* was in leafs but *Q.p.* leafless.

To upscale tree interception loss into the plot- and catchment-scale tree interception loss, further referred to as I_p and I_{ct} respectively, tree canopy area (A_c) as seen from space, was used as a scalar (Lubczynski, 2009). In that scaling, it is assumed that reference tree interception loss (I_r in L·T^{-1} referred to as per-species interception loss of a unit area of a canopy), does not differ between different sizes of trees (i.e., between different A_c) of the same species, in contrast to the volumes of intercepted water that depend on the tree canopy size; as such, for this study, it was assumed that $I_r = I_m$ per-species.

For the plot upscaling of tree interception loss, two quadratic 1-ha species-homogeneous areas of *Q.i.* and *Q.p.*, of approximately the same canopy coverage (~20%) were selected in the Sardon catchment (Fig. 1). The spatial upscaling in the two plots and also in the whole Sardon catchment, was done in four steps. First, the I_r was defined per species, per annum and per five characteristic tree interception loss assessment periods defined on the base of climatic seasonality and leaf status of *Q.p.* only as *Q.i.* is evergreen; for the sake of simplicity, in all simulated years, the interception loss assessment periods were assumed the same as follow: a) December-February (DJF), winter – *Q.p.* leafless; b) March-April (MA); early spring – *Q.p.* still leafless, although at the end, new leaves start to emerge: c) May-July (MJJ); late spring towards begin of a summer – *Q.p.* in leaf; d) August-September (AS), late summer begin of an autumn – *Q.p.* in leaf; and e) October-November (ON) – late autumn – *Q.p.* still in leaf although at the end starts dropping leaves. Second, the classified per species, tree canopy areas in the two plots and in the whole catchment, were defined using remote sensing procedures as explained above and following Reyes-Acosta and Lubczynski (2013). Third, the volumetric tree interception losses (L^3·T^{-1}) were estimated by multiplying the remote sensing defined canopy projection areas by the corresponding, experimentally defined I_r per species in respective interception loss assessment periods. Finally, in the fourth step, the volumetric tree interception losses were summed up per plots of 1-ha and per Sardon catchment area, and divided by respective plot or catchment areas within each interception loss assessment period and per annum.

It is acknowledged that interception loss measured at only one tree per species, might not sufficiently take into account eventual, differences in I_r between trees of the same species but different A_c. This limited amount of tree samplings to support the assumption that species-specific I_r is independent of tree size, was dictated by financial and logistical constrains of this study. Nevertheless, despite these limitations, it will be shown that the monitoring of only one tree per species to define I_r was sufficient, and credible because of predicted negligible interception loss variability within each species type, deduced based on estimated low LAI variability between trees of different sizes but the same species type (see below) and based on other studies investigations. The low variability of tree interception loss within given species type, is addressed by various researchers; for example: i) Mateos and Schnabel (2001) found an average standard deviation of tree interception loss of only 4% of rainfall among four different sizes of *Q.i.* trees in ~20 km northeast of the city of Cáceres in Extremadura (western Spain) and besides these small differences were due to tree pruning only; other characteristics of tree structure e.g., height, age, LAI were ignored in that study; ii) Moreno et al. (2001)

documented measured tree interception loss variation of 2.2% of rainfall per 1 $m^2 \cdot m^{-2}$ of LAI variation in four *Q.p.* dominated forest plots in the '*Sierra de Gata*', central-western Spain; and iii) Morán et al. (2008) documented *Q.p.* 2.3% of tree interception loss variation per 1 $m^2 \cdot m^{-2}$ of LAI at the 'Rinconada experimental catchment' ~50 km SW of Salamanca (western Spain).

For the temporal extrapolation of tree interception loss, the calibrated and validated revised analytical model (Gash et al., 1995) was used to simulate tree interception loss using the daily rainfall. The temporal extrapolation was done under the assumptions: (i) crown coverage change was negligible throughout the five-simulated years; and (ii) the I_r defined experimentally on the two species was applicable per-species, for other trees of the Sardon catchment.

The presented methodology of spatial and temporal (spatio-temporal) upscaling of the tree interception loss allows for quantification of tree interception loss at any spatial-scale (e.g., any size of the plot or catchment) and in any temporal-scale (e.g., for any day, week, month etc.). As example of the proposed methodology, the spatio-temporal upscaling was done and presented in $mm \cdot d^{-1}$ in squared grid of 1 ha, for annual mean values of HY2012 and HY2013 and also for five interception loss assessment periods of both years.

4. Results and discussion

4.1. Rainfall

In the two years of the observation period, the hydrological year 2012 (HY2012) was dry with only 335 mm of rainfall (*P*) and 2013 (HY2013) was moderately wet with 672 mm of *P*. As the study area falls in the relatively high-altitude highlands (733–860 m a.s.l.), like the majority of Iberian Peninsula, the annual rainfall with the long-term mean of 589 $mm \cdot y^{-1}$, is also typical for the Spanish *meseta* region i.e., with its typical range of 400–600 $mm \cdot y^{-1}$ (Alcalá and Custodio, 2014). A total of 52 discrete rainfall events (≥0.6 mm) were recorded in the HY2012 vs. 74 in the HY2013. The average (median) event-based rainfall amount, duration and intensity of rainfall in the HY2012 were 5.8 (3.7) mm, 7 h 21 min (4 h 20 min) and 1.3 (0.9) mm h^{-1}, respectively. Corresponding values in the HY2013 were 8.5 (3.8) mm, 10 h 19 min (5 h 5 min) and 2.0 (0.7) mm h^{-1} (Table 2). The average time between successive events in the rainy seasons within the two investigated years, was 90 (±110) h i.e., approximately two events per week. The frequency distribution of event size, rainfall intensity, and duration for the study period are shown in Fig. 3. There was no significant difference between the HY2012 and the HY2013 for any of these rainfall characteristics (p-value > 0.05, Mann-Whitney test). Most of the rainfall events (57%) were ≤5 mm, which covered 16% of total rainfall while the rainfall events of ≤10 mm represented majority (82%) of rainfall events (Fig. 3a), although covered only 42% of the total rainfall amount. The duration of most rainfall events (78%) was ≤10 h (Fig. 3b) and the intensity of most rainfall events (87%) was low (≤2 $mm \cdot h^{-1}$) (Fig. 3c). Such frequent and low intensity rainfall which is typical for Mediterranean climate (MIMAM, 2000) may enhance tree interception loss.

The rainfall pattern in the study area is highly temporally variable. The monthly rainfall during the 2-year study (Fig. 4) varied from zero in August 2013 to 149 mm in March 2013. In 2012, the driest and the wettest months were March and April with rainfall of 3 and 77 mm, respectively. The monthly peaks could exceed 100 mm in any of the nine months from September to May, as per continuous logging carried out since October 1993 (Hassan et al., 2014), while June to August were dry months.

The computed RIA shows that about 90% rainfall occurred within 35° and predominantly between 10 and 25° (Fig. 5). This indicates that the effects of wind-driven rainfall on the throughfall is (much) lower compared to the other similar studies (e.g., David et al., 2006; Pereira et al., 2009a; Xiao et al., 2000a). Moreover, rainfall concentration area (*L*) and rain-shadow area (*L'*) calculated

Table 2
Statistical parameters of rainfall events ≥0.6 mm (n = 126) during two hydrological years (HY2012 and HY2013).

Parameters	Event rainfall (mm)		Duration (h:min)		Intensity ($mm \cdot h^{-1}$)	
	HY2012	HY2013	HY2012	HY2013	HY2012	HY2013
Mean	5.8	8.5	7:21	10:19	1.3	2.0
Median	3.7	3.8	4:20	5:05	0.9	0.7
Standard Deviation	6.3	11.3	9:26	13:16	1.6	4.4
Range	0.6–32.3	0.8–60.9	0:30–48:20	0:20–65:00	0.2–10.5	0.2–27.7
Total	304	628	382:00	763:25		

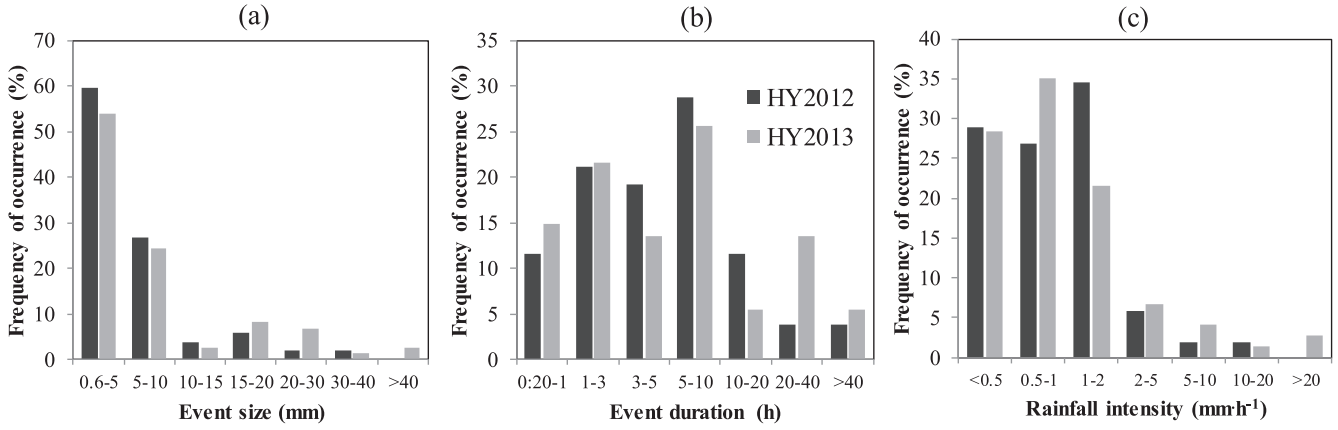

Fig. 3. Frequency distribution of: (a) amount; (b) duration; and (c) intensity of rainfall events in the two hydrologic years of the measurements from 1 October 2011 to 30 September 2013.

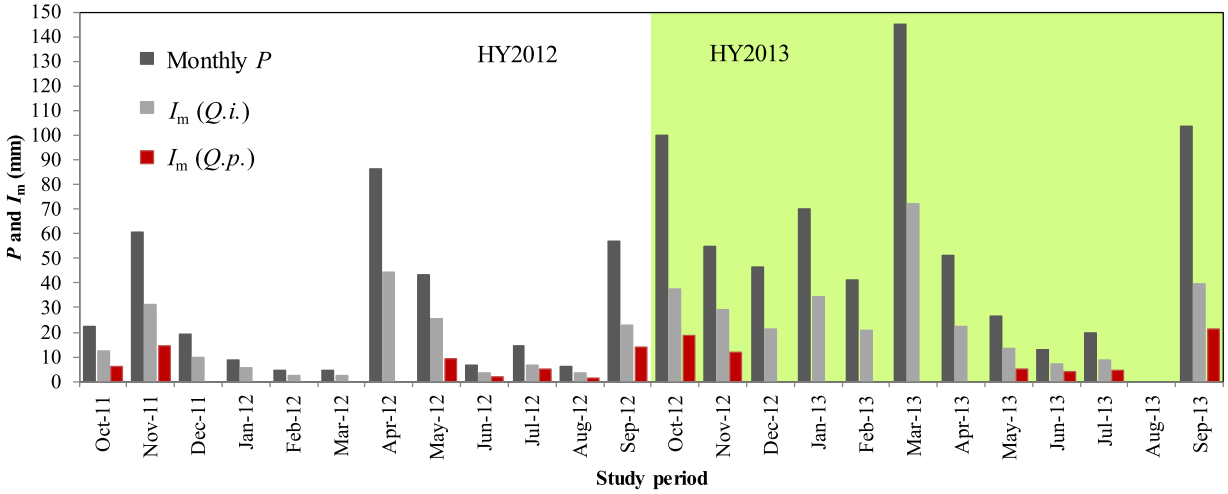

Fig. 4. Monthly gross rainfall and measured tree interception losses of *Quercus ilex* (*Q.i.*) and *Quercus pyrenaica* (*Q.p.*) oaks, during the 2-year study period. (For interpretation of the references to colour in this figure legend, the reader is referred to the web version of this article.)

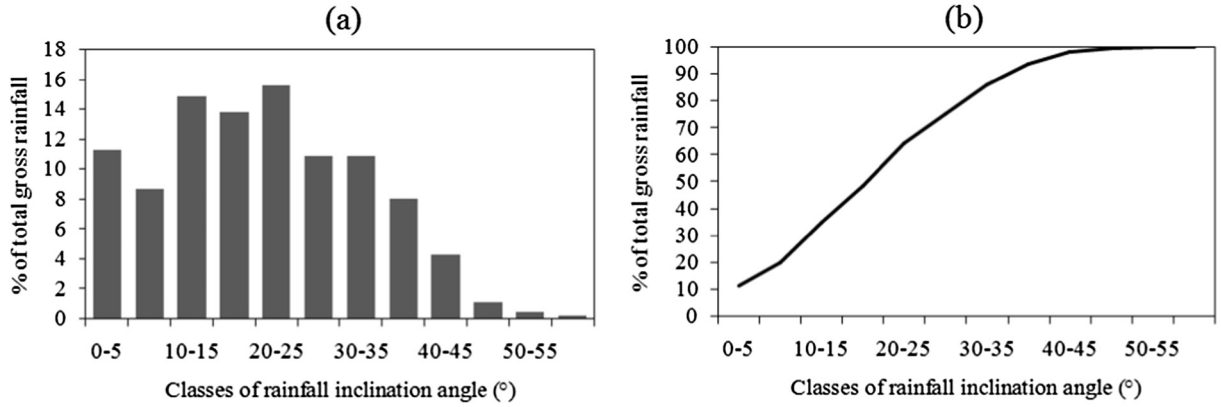

Fig. 5. Percentage of gross rainfall for different classes of rainfall inclination angle from 1 October 2011 to 30 September 2013: a) per each class; and b) as cumulative values.

with the RIA and crown heights on its windward and leeward sides (David et al., 2006), showed quite low values, i.e., median *L* of 0.3 m for *Q.i.* and 0.4 m for *Q.p.* and median *L′* of 1.4 m for *Q.i.* and 1.5 m for *Q.p*. This further supports our assumption that the wind-driven rainfall does not have large impact upon the estimation of tree interception loss in the Sardon catchment study area.

4.2. Stemflow, throughfall and derived tree interception loss

The measured stemflow (*Sf*) and throughfall (*Tf*) totals for the two study years, are presented in Table 3. The *Sf* during the study period was very small (<0.5 mm) and therefore was neglected. *Sf* usually represents less than 2% of the canopy water balance, although in extreme cases it can amount up to 12% of *P* in oak savannah forest in the Mediterranean climate (Levia and Frost, 2003; Llorens and Domingo, 2007). The very low *Sf* for both *Q.i.* and *Q.p.*, might be mainly because of horizontal or below horizontal branches of the trees (cf. Herwitz, 1987; Murakami, 2009) and low RIA in this study area.

The *Tf* differed between the two species (Table 3) and also between the two years. The larger *Tf* fraction (% of *P*) of the *Q.p.* than *Q.i.* is in line with the lower LAI and its deciduous nature, so temporally leafless status. The larger *Tf* of both *Q.i.* and *Q.p.* in HY2013 than in HY2012, is likely attributed to higher rainfall intensity in HY2013 than in HY2012 (Table 2).

The spatial distribution of *Tf* in each investigated tree during the 2-year experimental period is presented in Fig. 6. The *Tf* in *Q.p.* showed little variation between SW and NE gauges, to nearly no variation between NW and SE gauges, each receiving ~870 mm of *Tf* within the 2-year measurements. The *Tf* in *Q.i.* was the lowest for the NE (~400 mm) and highest for the SW gauges (~600 mm), while it varied little for the NW and SE gauges (Fig. 6). Overall, the

Table 3
Amounts of gross rainfall (*P*), throughfall (*Tf*), stemflow (*Sf*) and derived estimates of tree interception loss (I_m) during two hydrological years of measuring campaigns; *Tf* is mean ± SD of four tipping buckets; values in brackets represent fractional percentages of rainfall.

	P (mm)	*Quercus ilex*			*Quercus pyrenaica*		
		Tf (mm)	*Sf* (mm)	I_m (mm)	*Tf* (mm)	*Sf* (mm)	I_m (mm)
HY2012	335	165 ± 31 (49.3 ± 9.3)	0.32 (0.10)	170 (50.7)	276 ± 9 (83.4 ± 2.7)	0.04 (0.012)	53 (15.8)
HY2013	672	365 ± 72 (54.3 ± 10.7)	0.47 (0.07)	307 (45.7)	600 ± 14 (89.3 ± 2.1)	0.06 (0.009)	66 (9.8)
Annual mean	504	265 ± 52 (52.6 ± 10.2)	0.39 (0.08)	239 (47.4)	438 ± 12 (87.0 ± 2.3)	0.05 (0.010)	60 (11.8)

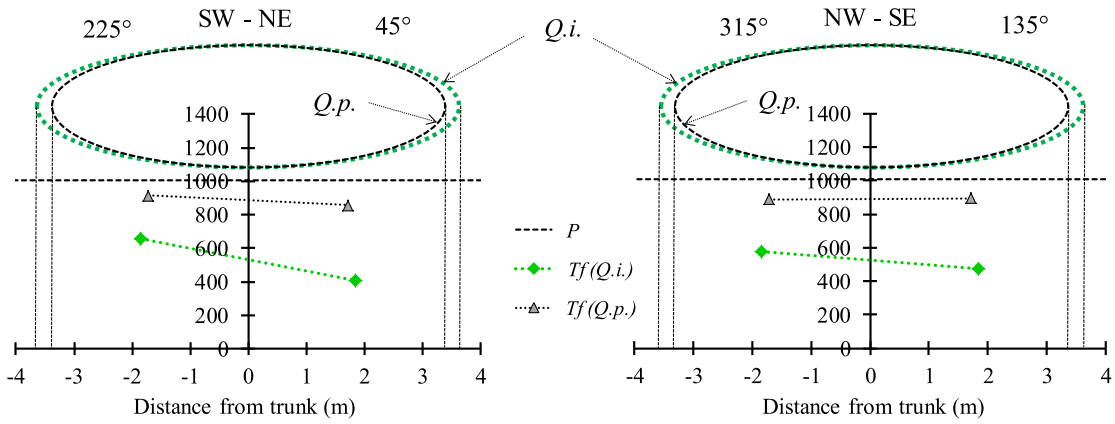

Fig. 6. Spatial distribution of throughfall (*Tf*) over 2-year experimental period, on the SW – NE (azimuth 225° and 45°) and NW – SE (azimuth 315° and 135°) directions centered at the tree trunk; the green and black ellipses represent the side view of the *Q.i.* and *Q.p.* canopy, respectively; values on the vertical axes refer to throughfall (mm); vertical dashed lines are projections of crown edges of *Quercus ilex* (*Q.i.*) and *Quercus pyrenaica* (*Q.p.*); and horizontal dashed line represents gross rainfall over 2-year study period (1007 mm). (For interpretation of the references to colour in this figure legend, the reader is referred to the web version of this article.)

spatial variation of throughfall (*Tf*) in this study is low to very low and is much lower as compared to the other studies in similar environmental conditions where such variability was much higher, even incidentally recording *Tf* in excess of gross rainfall (e.g., David et al., 2006). Therefore the tree interception loss (I_m, mm) was estimated as the difference between the measured rainfall (*P*, mm) and the arithmetic mean *Tf* (mm) of four tipping buckets and *Sf* (mm). The measured *Q.i.* and *Q.p.* tree interception losses (I_m) on monthly basis are presented in Fig. 4 and on yearly basis in Table 3. Because rainfall input was the same for both tree species and *Sf* proved to be very small, the higher tree interception loss of *Q.i.* is attributed to the higher leaf density, so to larger LAI and evergreen nature of the *Q.i.* tree.

The relationships between rainfall (*P*) and tree interception loss (I_m) for the *Q.i.* and the *Q.p.* trees are presented in Fig. 7a and b respectively. In both cases, the relationships between I_m and *P* were very strong ($R^2 > 0.9$) indicating the substantial evaporation from the wetted canopy. The higher canopy storage capacity of *Q.i.*, was partly responsible for its larger slope, so larger I_m increment with given *P* than *Q.p.* As a result of that, the relative tree interception losses in *Q.i.* for <5 mm·event^{-1} of rainfall were high, i.e., 66% of *P*; for 5–35 mm·event^{-1}, medium, i.e., 46% of *P*; and relatively low for >35 mm·event^{-1}, i.e., 32% of *P*. For *Q.p.* leafed period, the relative tree interception losses were generally lower, i.e.: for events <5 mm, 33%, for events 5–35 mm, 22% and for events >35 mm, 20%.

The 2-year *Q.i.* relative tree interception loss was 47.4% of *P*, with 50.7% of *P* in the first dry year and 45.7% in the second medium wet year. These *Q.i.* values were generally larger than in other similar, tree-scale studies such as in: i) Calabuig et al. (1978), who documented 37% of *P* in three *Q.i.* trees near Salamanca, Spain; (ii) Pereira et al. (2009a), who documented 30% of *P* by three *Q.i.* trees at the 'Herdade da Mitra' near Évora in southern Portugal with mean rainfall of 665 mm·y^{-1} but 21% canopy cover area and tree density of 35–45 stems·ha^{-1} (larger than in our study area); and (iii) Mateos and Schnabel (2001), who documented 30% of *P* in four *Q.i.* trees, in area with a tree density of 15 stems·ha^{-1} and 8% canopy cover in a Spanish *dehesa*. The larger relative tree interception loss of *Q.i.* in this study might be because of very low tree density (13 stems·ha^{-1} and 7% of canopy cover) implying wind-driven microclimatic conditions such as for example lower rainfall intensity or others related for example to higher wind speed and therefore possibly larger evaporation from the wet canopy (David et al., 2006; Pereira et al., 2009b, 2016).

Although comparative data on the interception loss by isolated *Q.p.* trees appears to be very scarce, the *Q.p.* relative interception loss obtained throughout the two years of this study, i.e., 11.8% of *P* (15.8% of *P* in the first dry year and 9.8% in the second medium

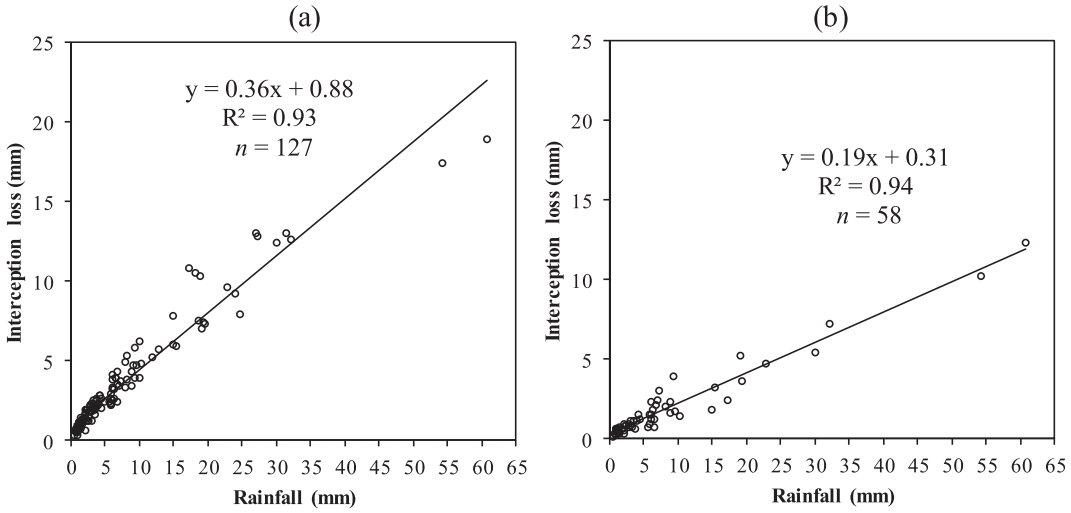

Fig. 7. The measured tree interception losses versus corresponding rainfall events for: a) *Quercus ilex*; and b) *Quercus pyrenaica* trees within the 2-year study period.

wet year) was comparable with other reported for *Q.p.* (or similar semi-deciduous species) dominated forests i.e., varied between 9 and 23% of *P* during leafless and leafed periods respectively (Morán et al., 2008; Moreno et al., 2001; Mużyło et al., 2012). The low relative interception loss by *Q.p.* found in this study and in other studies, is mainly attributed to the negligible rainfall interception loss during 5 months of leafless period (December–April).

4.3. Tree-scale canopy parameters

The canopy storage capacity (*S*) parameters as estimated using Jackson (1975) method, were 1.75 mm and 0.66 mm for *Q.i.* and *Q.p.*, respectively (Table 4). Higher *S* of the *Q.i.* is reflected by its higher LAI compared to *Q.p.* Determination of *S* by Jackson (1975) method can be a source of substantial error in modeling tree interception loss due to the subjective choice of event separation time (Llorens et al., 1997; van Dijk et al., 2015). To overcome this problem, taking a long gap, e.g., 6 h for the day-time and 12 h for night-time between successive events, as in this study and also proposed by Mużyło et al. (2012), is more appropriate than taking a short gap, e.g., 3-h between successive events used by many studies (e.g., Ghimire et al., 2012; Schellekens et al., 1999) as it reduces the model sensitivity to *S*, thus minimizes its potential error (Limousin et al., 2008). The estimated *S* values of this study are in the range of *S* values as in similar tree interception loss studies such as by Pereira et al. (2009a), who reported *S* = 1.16 mm for two *Q.i.* trees near Évora, in southern Portugal and by Limousin et al. (2008), with *S* values of 2.6 and 1.7 mm for natural (5464 stems·ha^{-1}, LAI 3.1) and thinned stands (2964 stems·ha^{-1}, LAI 1.6) respectively.

Canopy cover fraction *c* of this study (0.69 and 0.26 for *Q.i.* and *Q.p.* respectively) is rather incomparable with *c* in other studies, as majority of other tree interception loss modelling studies, defined *c* at the stand-scale, not at the tree-scale. An exception was David et al. (2006), who documented gap fraction at a *Q.i.* tree in MITRA I of 'Herdade da Mitra' site (286 ha) in southern Portugal as 0.2, (i.e., *c* = 0.8).

4.4. Modelling results

The total number of rainfall events (*n*) measured at the two trees during the study period was divided into two subsets, i.e., subset-1 of HY2012 (*Q.i.*, *n* = 52; *Q.p.*, *n* = 28) for model calibration and sub-set 2 of HY2013 (*Q.i.*, *n* = 74; *Q.p.*, *n* = 29) for model validation. The lower *n* for *Q.p.* than for *Q.i.* in both years is because for modelling purpose of leafless *Q.p.*, the 5-months rainfall from December to April, was not considered. The revised Gash analytical interception loss model requires the relative evaporation rate $\bar{E}/\bar{R}$, i.e., the ratio of the mean evaporation rate to the mean rainfall rate for the hours when the canopy was saturated (Gash, 1979; Schellekens et al., 1999). An estimate of $\bar{E}/\bar{R}$ for *Q.i.* and *Q.p.* was obtained firstly from the linear regression of tree interception loss vs. rainfall (*Tf*-based, $\overline{E_{Tf}}$) (Gash, 1979) and secondly from Penman-Monteith equation (PM-based, $\overline{E_{PM}}$). The *Tf*-based approach resulted in $\bar{E}/\bar{R}$ values of 0.38 and 0.21 for the *Q.i.* and *Q.p.*, respectively. Combining the obtained $\bar{E}/\bar{R}$ with the median rainfall intensity falling onto a saturated canopy as calculated from calibration dataset ($\bar{R}$ = 1.67 and 1.97 mm·h^{-1} for *Q.i.* and *Q.p.*, respectively), yielded $\overline{E_{Tf}}$ of 0.63 and 0.42 mm·h^{-1} for the *Q.i.* and *Q.p.*, respectively. The PM-based approach with the canopy resistance (r_s) set to zero, yielded $\overline{E_{PM}}$ of 0.037 and 0.043 mm·h^{-1} for the *Q.i.* and *Q.p.*, respectively (Table 4).

Many studies of rainfall interception loss elsewhere have reported similarly large discrepancies between $\overline{E_{PM}}$ and $\overline{E_{Tf}}$ (e.g., Bruijnzeel et al., 1987; Dykes, 1997; Fan et al., 2014; Ghimire et al., 2012, 2017; Holwerda et al., 2012; Schellekens et al., 1999; Wallace and McJannet, 2008). The most commonly cited reasons include the application of the equation for momentum transfer of Thom (1975) in topographically complex terrain to derive the aerodynamic resistance in Penman-Monteith equation (Holwerda et al., 2012; van Dijk et al., 2015) but this does not readily apply to the present study area, which is relatively flat and smooth. Likewise, enhanced evaporation of rain droplets that are produced when raindrops hit the canopy has been invoked as a possible mechanism for high wet canopy evaporation rate (Murakami, 2006) but given the low rainfall intensities prevailing in the study area, this does not seem to explain the difference between $\overline{E_{PM}}$ and $\overline{E_{Tf}}$. The most likely explanation of the observed discrepancy between $\overline{E_{PM}}$ and $\overline{E_{Tf}}$ in this study area can be the uncertainty in the estimation of aerodynamic conductance by Thom (1975) approach, which is valid for closed canopies (e.g., dense forest, crop field etc.) over uniform, flat surfaces where effect of topography and vegetation on wind flow pattern is minimal (Teklehaimanot et al., 1991).

The revised version of the Gash model was run on an event basis using the respective canopy and climatic parameters for each tree as listed in the Table 4. The observed and predicted tree interception losses are summarized in Table 5 and presented in Fig. 8. In the first run of the Model A, $\overline{E_{Tf}}$ values were used to characterize wet canopy evaporation rate. The predicted tree interception losses (I_{Tf}), for *Q.i.* were only 3.5% larger and for *Q.p.* 5.5% smaller than the observed losses (I_m) with RMSE $\leq$0.7 mm. A much worse fit (RMSE $\geq$1.8 mm) between modeled (I_{PM}) and observed (I_m) tree interception losses was obtained when using $\overline{E_{PM}}$ in the Model B, which underestimated tree interception loss in the *Q.i.* by 47.6% and in *Q.p.* by 60%. As the performance of the Model A was much better compared to the Model B, the validation was carried out using the estimated canopy parameters and the $\overline{E_{Tf}}$. The predicted I_{Tf} for the validation dataset were in good agreement with I_m, with relative errors of $\leq$6.3% and RMSE of $\leq$1 mm. The calibrated and validated model was then used to estimate the tree interception loss during 5-year period (see below).

4.5. Upscaling the single tree interception loss into the plot- and catchment-scale

Within the Sardon catchment, a total of 102,748 trees were identified on a high resolution *QuickBird* image (20 August 2009) of 0.6 m and a *WorldView-II* image (14 December 2010) of 0.5 m (as modified after Reyes-Acosta and Lubczynski, 2013, Fig. 1) of

Table 4
Summary of canopy and climatic parameters used in the revised Gash's analytical model. *Q.i.* and *Q.p.* denote the *Quercus ilex* and *Quercus pyrenaica* respectively.

Experimental tree	Canopy parameters[a]			Climatic parameters[b]		
	S (mm)	*p* (–)	*c* (–)	$\bar{R}$ (mm·h^{-1})	$\overline{E_{PM}}$ (mm·h^{-1})	$\overline{E_{Tf}}$ (mm·h^{-1})
Q.i.	1.75	0.31	0.69	1.67	0.037	0.63
Q.p.	0.66	0.74	0.26	1.97	0.043	0.42

[a] Canopy parameters: *S* = canopy storage capacity; *p* = free throughfall coefficient; *c* = canopy cover fraction.
[b] Climatic parameters; $\bar{R}$ = median rainfall intensity falling onto a saturated canopy; $\overline{E_{PM}}$ = wet-canopy evaporation rate derived using the Penman-Monteith equation; $\overline{E_{Tf}}$ = throughfall-based estimate of wet-canopy evaporation rate.

Table 5
A comparison of measured (I_m, mm) and modelled annual rainfall interception losses (mm) for the two tree species, *Quercus ilex* and *Quercus pyrenaica*; Model A – interception loss (I_{Tf}) estimated using *Tf*-based wet-canopy evaporation rate ($\overline{E_{Tf}}$); Model B – interception loss (I_{PM}) estimated using P-M-based wet-canopy evaporation rate ($\overline{E_{PM}}$).

Component of interception loss	Calibration (HY2012)				Validation (HY2013)	
	Q.i.		*Q.p.*		*Q.i.*	*Q.p.*
	Model A	Model B	Model A	Model B	Model A	Model A
Gross rainfall (*P*, mm)	335	335	335	335	672	672
Total measured interception loss (I_m, mm)	170	170	55	55	307	64
Total modelled interception loss	176	89	52	22	322	68
Modelled – measured (% relative error)	3.5	−47.6	−5.5	−60	4.9	6.3
RMSE (mm)	0.7	2.8	0.6	1.8	1.0	0.7

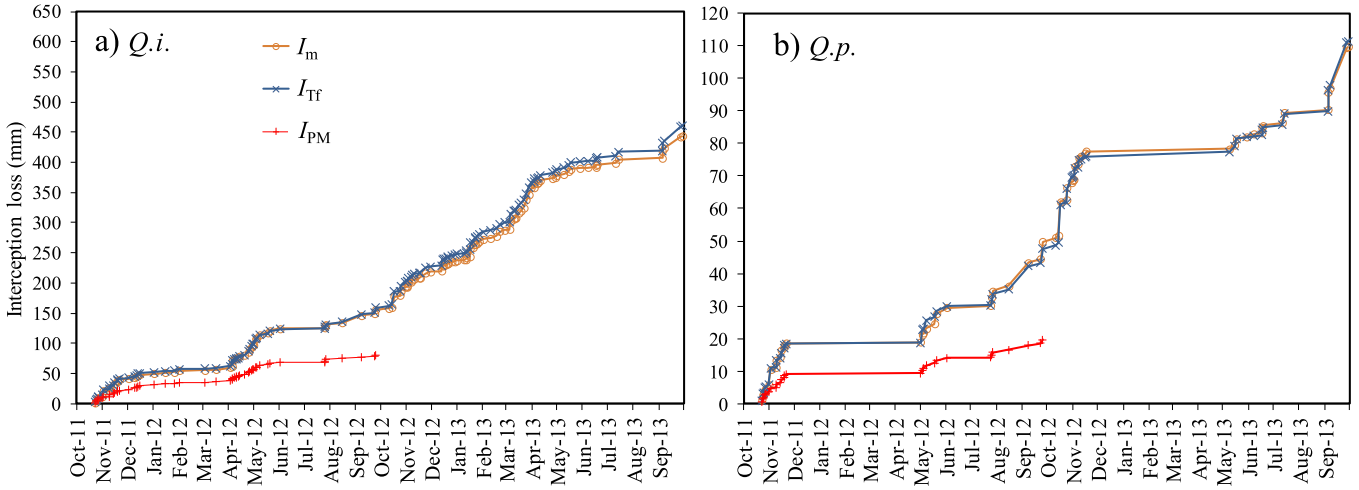

Fig. 8. Cumulative measured (I_m) and simulated tree interception losses (I_{Tf}, I_{PM}) for both calibration and validation periods for: a) *Quercus ilex* (*Q.i.*) and b) *Quercus pyrenaica* (*Q.p.*); the tree interception losses I_{Tf} and I_{PM} are the results of simulations using respective throughfall-based ($\overline{E_{Tf}}$) and Penman-Monteith based ($\overline{E_{PM}}$) average wet canopy evaporation rates as in Table 4. (For interpretation of the references to colour in this figure legend, the reader is referred to the web version of this article.)

which 20,097 were *Q.i.* and 82,651 *Q.p.* The mean catchment tree density was low, i.e., 13 stems·ha^{-1} and the catchment canopy cover 7%, comprising 3 stems·ha^{-1} of *Q.i.* (2% of the catchment area) and 10 stems·ha^{-1} of *Q.p.* (5% of catchment area) with a mean canopy areas of 60 (±25) m^2·tree^{-1} and 48 (±17) m^2·tree^{-1}, respectively. The species occurrence at the catchment scale is highly clustered (Fig. 9), i.e., mainly there are species-homogenous areas of either *Q.i.* or *Q.p.* growth and very rare areas with mixed species.

The comparison of structural and biometrical characteristics of the selected *Q.i.* and *Q.p.* experimental trees with the corresponding *Q.i.* and *Q.p.* means in homogeneous plots (location in Fig. 1d and e) and in the whole catchment, is presented in Table 6. The per-species differences between the biometrics of the selected experimental trees and the two plots and the whole catchment, are small, and within the range of standard deviations (SD) of the mean.

The spatial upscaling of tree interception loss at the plot (I_p) and at the catchment scale (I_{ct}) requires definition of the species-specific, temporally variable, reference tree interception (I_r) losses. These were assigned for *Q.i.* and *Q.p.* as independent of the canopy size based on interception loss measurement of one tree per species, each investigated using four throughfall and one stemflow gauges. More appropriate would be to investigate per-species I_r on more trees of different sizes and using more throughfall gauges per tree to test I_r dependence on canopy size and eventually on environmental conditions. Unfortunately, for logistical and instrumental-shortage reasons, we did not have such opportunity. However as mentioned earlier, the main objective of this study was not the widely investigated interception loss measurement of the *dehesa* oaks but presentation of the novel method of spatial upscaling of that interception loss. Besides, although the assumption of the I_r as independent on the canopy area involves some uncertainty, it will be shown that this uncertainty is quite low so that per-species variability of tree interception loss between trees of different sizes, is low.

Tree interception loss is known to be closely and positively related to the leaf area index (LAI) for a given climate (Gómez et al., 2001; van Dijk and Bruijnzeel, 2001). In the Sardon study area, the LAI variability was assessed to predict per-species, tree interception loss variability of *Q.i.* and *Q.p.* The LAI was defined experimentally, by field measurements and through its relation with NDVI (Qi et al., 2000) obtained by remote sensing image processing. In the Sardon study area, *Q.i.* and *Q.p.* had a very narrow LAI variability ranges; according to: i) experimental field measurements, LAI of *Q.i.* varied from 2.0 to 3.9 m^2·m^{-2} and *Q.p.* from 1.5 to 3.0 m^2·m^{-2} (Fig. 10a,b); ii) NDVI estimates, 97% of LAI estimates of *Q.i.* varied from 1.2 to 2.8 m^2·m^{-2} and 98% of *Q.p.* varied from 1.4 to 2.6 m^2·m^{-2} (Fig. 10c-f); the low LAI variability per-species is also confirmed by relatively low coefficients of variation, 20% for *Q.i.* and 16% for *Q.p.* Moreover, the LAI of the trees selected for interception loss measurements were, 2.1 m^2·m^{-2} for *Q.i.* and 1.6 m^2·m^{-2} for *Q.p.*, as measured on 7–8 September 2010, so close to the mean of the sampled tree populations in the two plots and to the mean of the whole catchment scale and well within the range of low standard deviations of the means (Table 6), i.e., 0.4 and 0.3 m^2·m^{-2} for *Q.i.* and *Q.p.* respectively.

By comparing field with NDVI-derived estimates of LAI, it can be observed that field estimates are generally larger, although the most important for this LAI variability-proof-analysis, are not the absolute values that could differ depending on the method applied, but the variability ranges that are comparable. Considering that all the ranges of LAI estimates in the Sardon study area were

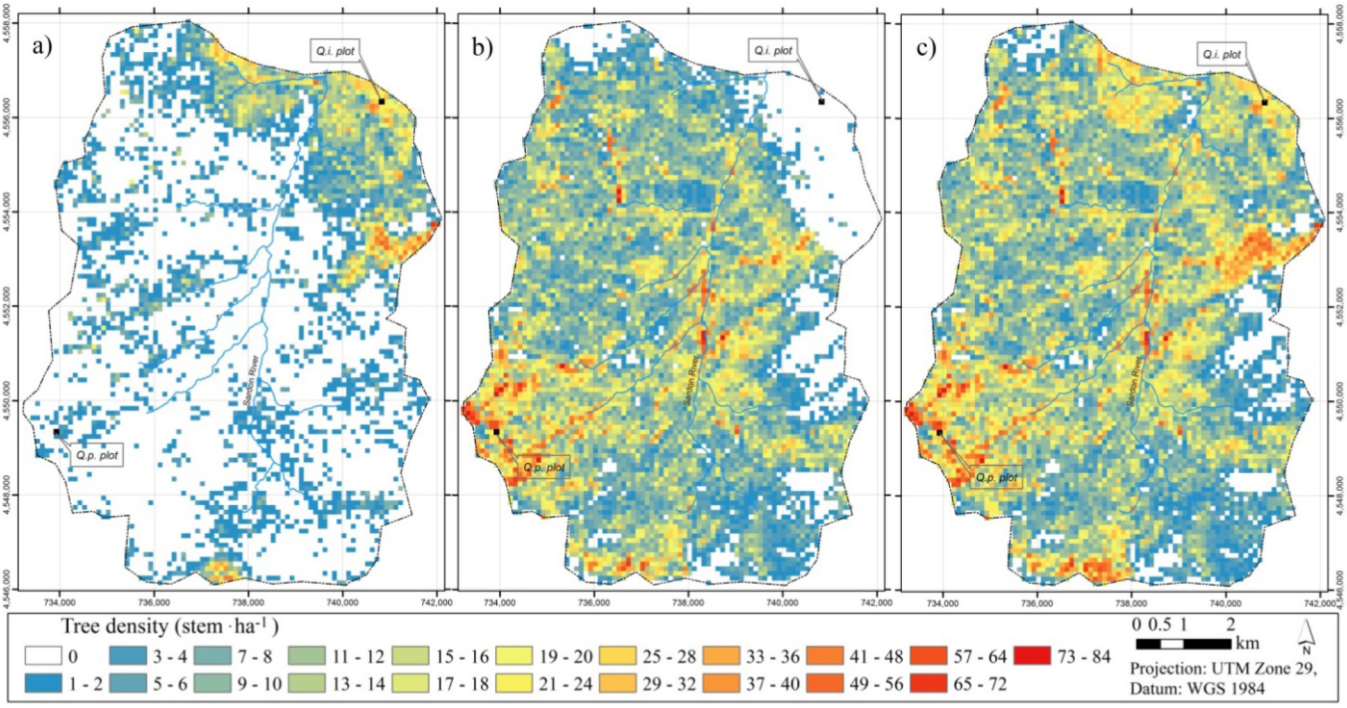

Fig. 9. Tree density map of: a) *Quercus ilex*; b) *Quercus pyrenaica*; and c) all trees; the investigated homogeneous *Q.i.* and *Q.p.* plots are shown by black squares (the maps are modified after Reyes-Acosta and Lubczynski (2013)). (For interpretation of the references to colour in this figure legend, the reader is referred to the web version of this article.)

Table 6
Comparison between structural and biometrical characteristics of experimental *Quercus ilex* (*Q.i.*) and *Quercus pyrenaica* (*Q.p.*) trees, experimental plots and per-species catchment means and standard deviations (in brackets); LAI – leaf area index; DBH – diameter at breast height; SD – standard deviation; catchment means of tree heights, canopy areas, and DBH were obtained from sampling survey by Reyes-Acosta and Lubczynski (2013) whereas catchment means of LAI were obtained from the direct field LAI measurements and remote sensing based approach as in Fig. 10.

Tree characteristics	*Quercus ilex*			*Quercus pyrenaica*		
	Experimental tree	Experimental plot mean (±SD)	Catchment mean (±SD)	Experimental tree	Experimental plot mean (±SD)	Catchment mean (±SD)
Height (m)	7.2	7.6 (±0.9)	7.7 (±0.7)	7.6	7.3 (±1.0)	8.2 (±1.0)
Canopy projection area (m^2)	43	62 (±24)	60 (±25)	37	33 (±12)	48 (±17)
DBH (m)	0.32	0.46 (±0.16)	0.44 (±0.15)	0.27	0.25 (±0.06)	0.34 (±0.10)
LAI ($m^2 \cdot m^{-2}$)	2.1	2.0 (±0.2)	2.0 (±0.4)	1.6	1.9 (±0.3)	1.9 (±0.3)

<2 $m^2 \cdot m^{-2}$, the remaining is the question, what are the per-species, I_r changes corresponding to 1 $m^2 \cdot m^{-2}$ of LAI change. For *Q.p.* this was well defined; in similar environmental condition as the Sardon catchment, the I_r variability was in order of only ~2.2% per 1 $m^2 \cdot m^{-2}$ of LAI change (Morán et al., 2008; Moreno et al., 2001); considering that *Q.p.* LAI in the Sardon Catchment ranges <1.5 $m^2 \cdot m^{-2}$, the estimated *Q.p.* I_r variability would be ≤3.3%. Unfortunately, to our knowledge, there are no similar published studies for *Q.i.*; however, considering that the *Q.i.* is an evergreen species and has low LAI variability not only temporal but also spatial at the canopy scale (Mateos and Schnabel, 2001), the expected per-species I_r variability between *Q.i.* of different sizes, is also low.

Per-species and per-annum analysis of I_r within five characteristic assessment periods is presented in Table 7. For *Q.i.*, in dry year 2012, the I_r varied from 0.20 mm·d^{-1} in winter months (DJF) (P = 0.36 mm·d^{-1}) to 0.77 mm·d^{-1} in early spring (MA) (P = 1.49 mm·d^{-1}). In the medium-wet year 2013, the I_r of *Q.i.* was the lowest, 0.32 mm·d^{-1}, in late spring-summer (MJJ) (P = 0.64 mm·d^{-1}, the lowest) and the largest, 1.55 mm·d^{-1}, in early spring (MA) (P = 3.21 mm·d^{-1}). In contrast, the I_r of *Q.p.* was primarily dependent on the leaf status. For five month of leafless period (DJFMA), the I_r of *Q.p.* was negligible. In the remaining seven months, the I_r of *Q.p.* exhibited similar relation with P as *Q.i.*, but in all the assessment periods, the I_r of *Q.p.* was approximately twice lower than in *Q.i.* despite receiving the same rainfall. Remarkable is that we did not find any relationship between I_r and *PET* (Table 7).

For the spatio-temporal upscaling of the tree interception loss at the plot scale (I_p), the seasonally varying I_r as listed in Table 7 and corresponding fractional canopy coverages were used. As the two *Q.i.* and *Q.p.* selected plots are species-homogeneous, and both have ~20% canopy coverage, their seasonal I_p variability is equal to 0.2I_r, while the per-species I_r are listed in Table 7. The yearly I_p for the *Q.i.* plot were, 34 mm (10.1% of P) and 61 mm (9.1% of P) for HY2012 and HY2013, respectively. The yearly I_p for the *Q.p.* plot were 10.6 mm (3.2% of P) and 13.2 mm (2.0% of P) for HY2012 and HY2013, respectively. It is remarkable that despite nearly the same total canopy cover in both plots (~20%), the yearly I_p of *Q.i.* and *Q.p.*, were so much different, i.e., yearly I_p of *Q.i.* was 3.2-times larger in dry HY2012 than in *Q.p.* and 4.6-times larger in medium-wet HY2013. These differences are mainly due to leafless periods of *Q.p.* (i.e., negligible interception loss in leafless periods; Table 7).

More complex was spatio-temporal catchment scaling of the tree interception loss (I_{ct}), because of spatially variable associations

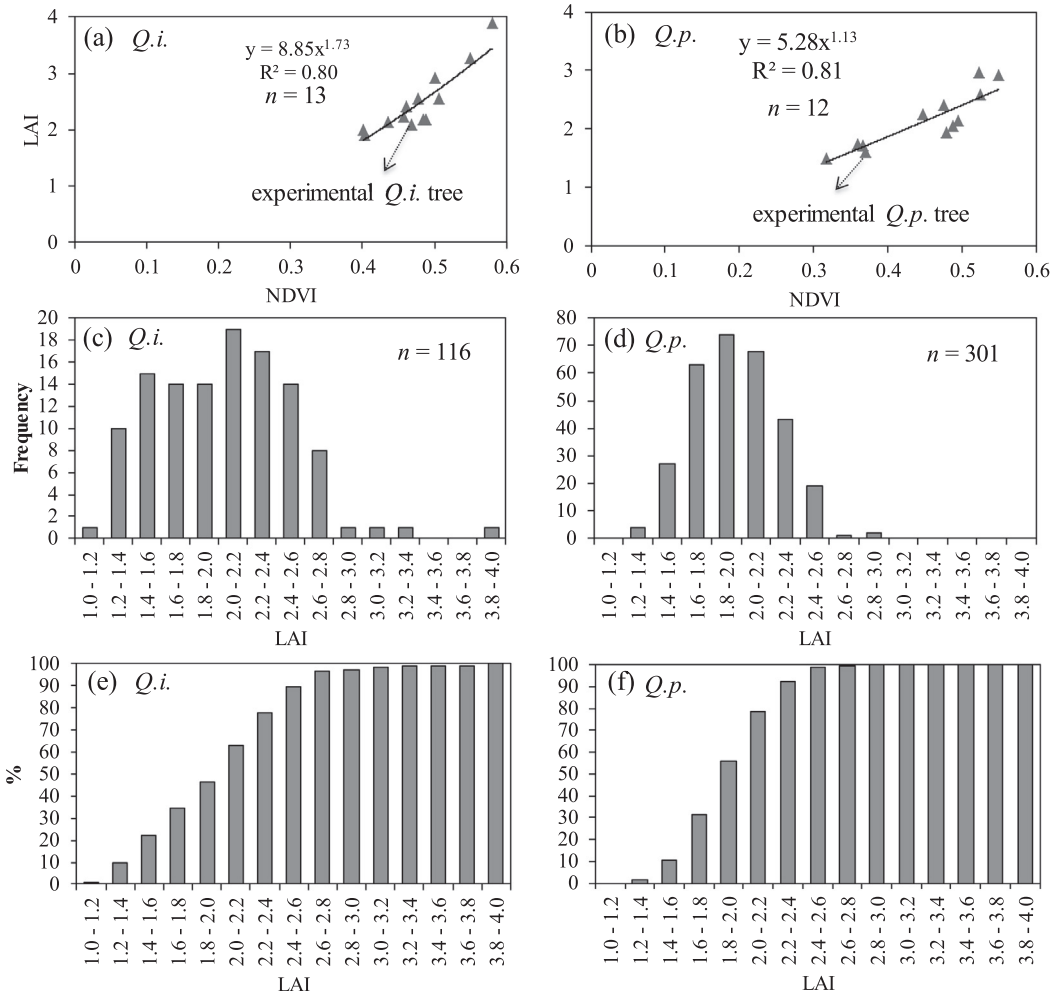

Fig. 10. Relation between normalized difference vegetation index (NDVI) from *QuickBird* multispectral image and field-measured leaf area index (LAI) for: a) *Quercus ilex* (*Q.i.*) and b) *Quercus pyrenaica* (*Q.p.*); the LAI frequency histograms for: c) *Q.i.*; and d) *Q.p.*; and the LAI frequency cumulatives for: e) *Q.i.*; and f) *Q.p.*

Table 7
Catchment-scale tree interception loss (I_{ct}), gross rainfall (P), potential evapotranspiration (PET) and reference evaporation (I_r) during characteristic assessment periods within the 2-year measurements.

Period	HY2012						HY2013					
	P	PET	I_r		I_{ct}		P	PET	I_r		I_{ct}	
	(mm·d^{-1})	(mm·d^{-1})	*Q.i.* (mm·d^{-1})	*Q.p.* (mm·d^{-1})	(mm·d^{-1})	(% of P)	(mm·d^{-1})	(mm·d^{-1})	*Q.i.* (mm·d^{-1})	*Q.p.* (mm·d^{-1})	(mm·d^{-1})	(% of P)
Dec-Feb	0.36	0.94	0.20	0	0.0031	0.9	1.76	1.10	0.85	0	0.0128	0.7
Mar-Apr	1.49	2.20	0.77	0	0.0116	0.8	3.21	2.63	1.55	0	0.0234	0.7
May-Jul	0.70	4.55	0.38	0.18	0.0150	2.1	0.64	5.74	0.32	0.15	0.0121	1.9
Aug-Sep	1.04	4.09	0.43	0.26	0.0193	1.9	1.70	5.28	0.65	0.35	0.0271	1.6
Oct-Nov	1.36	1.62	0.71	0.34	0.0277	2.0	2.54	1.78	1.10	0.51	0.0416	1.6
Annual (mm·d^{-1})	0.92	2.70	0.47	0.15	0.0143	1.6	1.84	3.34	0.84	0.18	0.0216	1.2
Annual (mm)	335		170	53	5.2	1.6	672		307	66	7.9	1.2

between the two species. Nevertheless, this was accomplished through the use of high resolution multispectral imagery as described earlier (Section 3.9). The I_{ct}, similarly to I_p, depends on: i) tree species type and related leaf status; ii) tree size, and age (canopy area, LAI etc.); iii) tree density and distribution; and iv) surrounding environmental conditions. In order to present spatio-temporal variability of I_{ct} and also to illustrate the applicability of our scaling method, the I_{ct} are presented in 100 × 100 m (1 ha) grids as the means of HY2012 and HY2013 in Fig. 11a and b respectively and within five characteristic I_{ct} assessment periods in each of the two analyzed years in Fig. 11c-l. The corresponding catchment I_{ct} are summarized in Table 7. The larger I_{ct} in medium-wet 2013 (Fig. 11b) than in dry 2012 (Fig. 11a) reflects substantially larger rainfall in 2013 (672 mm) than in 2012 (335 mm). During the five winter and early spring leafless periods (DJFMA), *Q.p.* trees were dormant, so the I_{ct} was entirely dependent on density and clustering of *Q.i.* trees and also on their I_r, larger in 2013 than in 2012 and larger during MA than during DJF months (Fig. 11c-f). In MJJ, the rain was low, but both, *Q.i.* and *Q.p.* trees were active, so the I_{ct} was the most spatially uniform and in contrast to other periods, was slightly larger (Table 7) in 2012 (Fig. 11g) than in 2013 (Fig. 11h). In other two characteristic

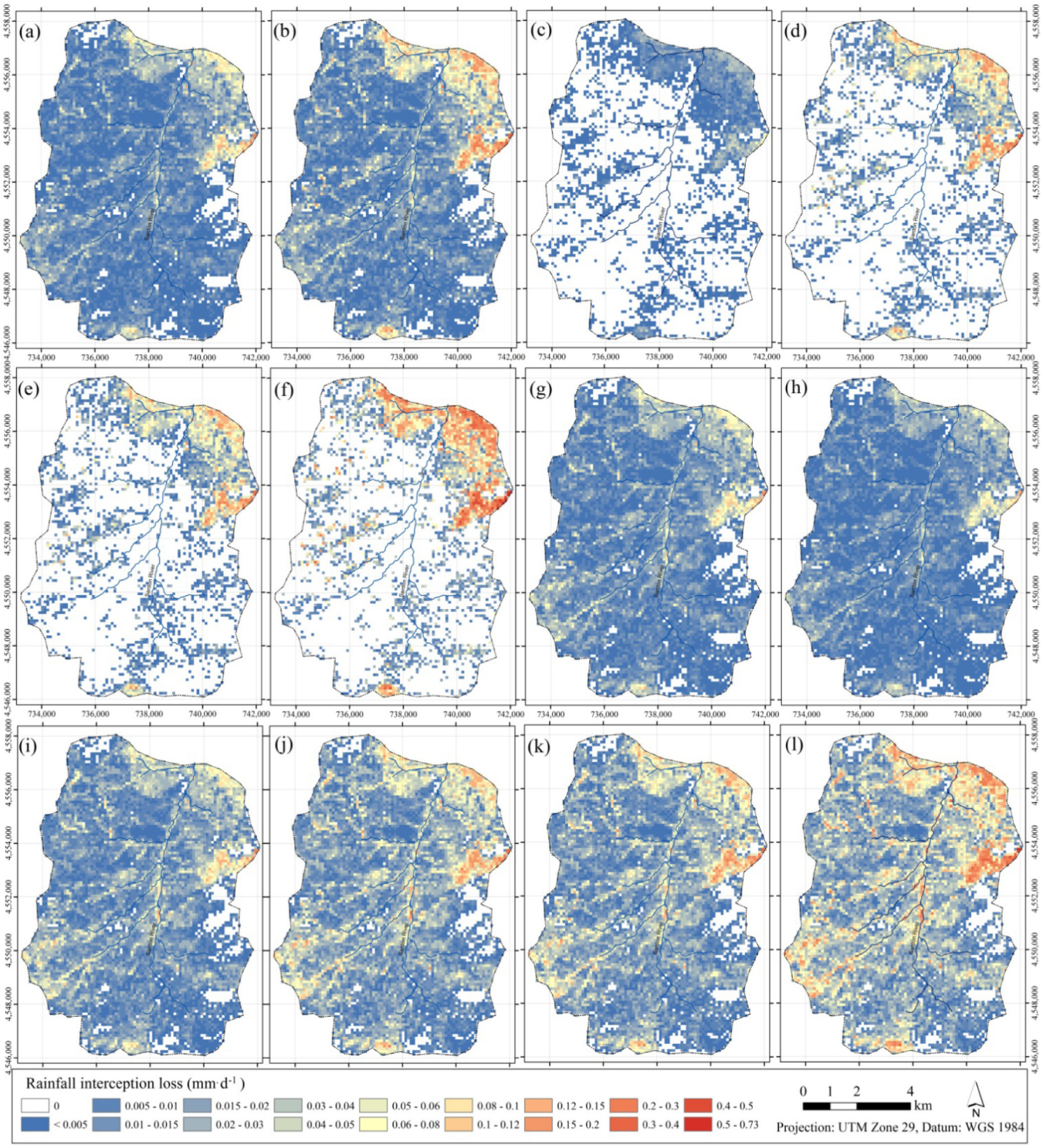

Fig. 11. Catchment tree interception loss (I_{ct}) maps of the Sardon catchment during:(a) HY2012-annual total; b) HY2013 - annual total; c) December – February (DJF) of HY2012; d) DJF of HY2013; e) March – April (MA) of HY2012; f) MA of HY2013; g) May – July (MJJ) of HY2012; h) MJJ of HY2013; i) August – September (AS) of HY2012; (j) AS of HY2013; (k) October – November (ON) of HY2012; and l) ON of HY2012 in mm·d^{-1}; all the tree interception loss maps were obtained by remote sensing upscaling of measured tree interception losses in the period from 1 October 2011 to 30 September 2013. (For interpretation of the references to colour in this figure legend, the reader is referred to the web version of this article.)

periods, i.e., AS (Fig. 11i,j) and ON (Fig. 11k,l), rainfall increased, so I_{ct} too, being larger in ON than in AS and larger in 2013 than in 2012 (Table 7). Considering similar PET conditions in the two years analyzed, the above analysis points at strong interception loss dependence on rainfall intensity and frequency i.e., low rainfall intensities and frequent occurrence of small rainfall events, enhance the tree interception loss. As the catchment is dominated by *Q.p.* (77% of canopy coverage), not only spatial but also seasonal variability is largely influenced by contributing interception loss of that species (Table 7). For example, in both years (HY2012 and HY2013), the largest rainfall was in months MA but the largest I_{ct} was in months ON when rainfall was lower than in MA, because in MA, the spatially dominant *Q.p.* was leafless, while in ON *Q.p.* was still in leaf contributing to I_{ct}. The annual I_{ct} during HY2012

and HY2013 were 5.2 and 7.9 mm, respectively (Table 7, Fig. 11a and b) while the relative I_{ct} during HY2012 and HY2013 were 1.6 and 1.2% of P, respectively.

The spatial interception losses, such as I_p or I_{ct}, are dependent on I_r and on per-species fractional canopy coverage. When comparing interception loss in different areas such as plots or catchments, various influencing factors have to be taken into account because the I_r depends on rainfall and on the characteristics of the sampled tree itself, while the fractional canopy coverage on environmental characteristics of a scaled area such as species composition, tree density, size and shape of canopies etc. Because of these complex dependencies, it was difficult to compare this study, spatial tree interception loss (two homogeneous plots, both with 20% canopy coverage and whole catchment with 7% canopy coverage) with spatial tree interception losses in other studies. Nevertheless, such attempt has been made, just to get idea on how the I_p and the I_{ct} of this study compare with the I_p of other studies (no I_{ct} of other study was available for comparison). For example, in two *Q.i.* dominated plots (MITRA I and MITRA II, 3 km away from each other) at 'Herdade da Mitra' research area (286 ha) of University of Évora, southern Portugal, Pereira et al. (2009a) documented relative I_p of 6.2% of P in a plot with 21% of canopy cover (MITRA II) and 9.0% in a plot with 39% of canopy cover (MITRA I). The I_p of *Q.i.* plot of our study was larger, because of larger I_r of the investigated *Q.i.* tree (47.4% of P) than I_r in their study (29.6% and 23% in MITRA II and I plots, respectively). In other *Q.i.* study, in Guadalperalón 35 ha plot of mixed evergreen *Q.i.* and *Quercus suber* located 20 km northeast of the city Cáceres in Extremadura, Spain, Mateos and Schnabel (2001) obtained relative I_p of 4% of P with 8% canopy cover. Their I_p, despite being lower, was comparable to the *Q.i.* plot of this study relatively to the canopy coverage (~10% of P with 20% canopy coverage). Considering spatial tree interception loss of *Q.p.*, to our knowledge there is no comparable study area, with similar to this study, tree density and climatic conditions. Because of different conditions, Morán et al. (2008) obtained relatively higher I_p of 12–19% of P in four small plots (99–125 m^2) of dense *Q.p.* dominated forest (density 1050–4475 stems·ha^{-1}) in 62 ha Rinconada experimental catchment in *Sierra de Tamames* in *Sistema Central* near Salamanca, Spain. Also Moreno et al. (2001) obtained higher I_p of 13–15% in four plots (close <15 km apart; plot size 0.5–0.94 ha) of dense *Q.p.* dominated forest (density 406–1043 stems·ha^{-1}) located in *Sierra de Gata* near Salamanca, Spain. The lower spatial *Q.p.* interception loss in this study area than in other study areas is mainly because of much lower fractional canopy cover, much drier, semi-arid climate and probably, because of the related longer (~5 months) leafless period. The dominance of *Q.p.* species in the Sardon catchment (Fig. 9) characterized by the low I_r and the low catchment tree density, (~7% canopy cover), are the main reasons of very low Sardon catchment interception loss (I_{ct}) (1–2% of P).

Fig. 12 is an example of temporal scaling (extrapolation), applying revised Gash analytical model simulation using the parameters listed in the Table 4. Because the study area receives typically two rainfall events per week, daily rainfall data was used to simulate tree interception loss for temporal extrapolation. The whole simulation period involves 2-year measurements (HY2012 and HY2013), 2-year backward Gash model simulation (HY2010 and HY2011) and 1-year forward simulation (HY2014). The mean annual rainfall in the analyzed 5-year period was 583 mm, which is higher than in the 2-year period of measurements (503 mm·y^{-1}). Fig. 12a shows monthly rainfall versus measured and temporally upscaled using revised analytical model (Gash et al., 1995), single tree interception losses (I_r), while Fig. 12b presents scaled up monthly variability of catchment tree interception loss (I_{ct}). For the 5-year simulation, the mean annual I_r was 303 mm (52% of P) and 59 mm (10% of P) for *Q.i.* and *Q.p.*, respectively while I_{ct} was 7.5 mm (1.3% of P). With the presented upscaling method, plot- or catchment-scale tree interception loss can be quantified on any day, week, month or year at an analyzed study area.

To the best of the authors' knowledge, this is the first study to upscale tree interception loss at the catchment-scale using ground measurements and object-attributes derived from the satellite

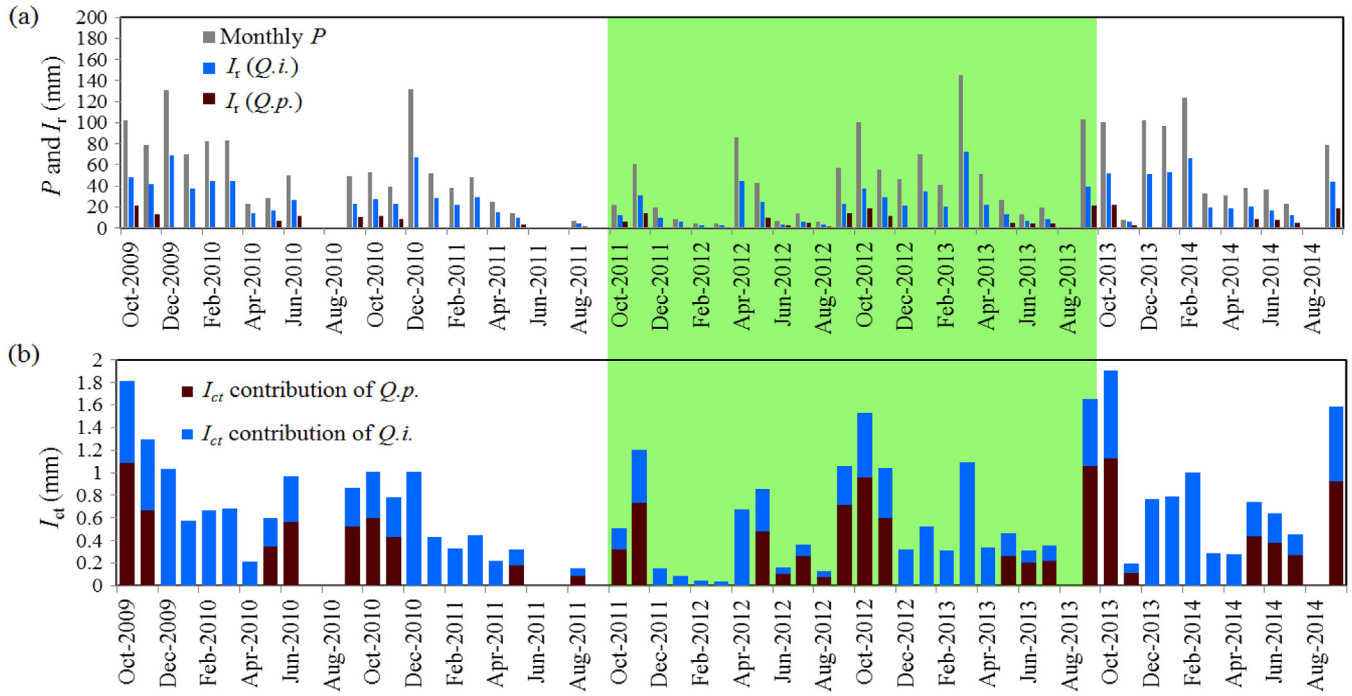

Fig. 12. Revised Gash's analytical model simulation of: a) single-tree, reference interception loss (I_r) from *Quercus ilex* (*Q.i.*) and *Quercus pyrenaica* (*Q.p.*); and b) upscaled, catchment tree interception loss (I_{ct}); note that the two colors represent individual contributions of the *Q.p.* and *Q.i.* species while the sum of the two, represents total catchment tree interception loss (I_{ct}); green shaded area represents the model calibration and validation period as in Fig. 4. (For interpretation of the references to colour in this figure legend, the reader is referred to the web version of this article.)

imagery. Although there are some important studies that evaluated interception loss at very large-scales e.g., regional- or global-scale using remote sensing products e.g., NDVI or LAI (e.g., Cui and Jia, 2014; Miralles et al., 2010; Nieschulze et al., 2009; Peng et al., 2009), the presented upscaling of the tree interception loss measurements, using object-attributes seems to be more effective and possibly more accurate than any other presented before, because: i) of its direct link with ground interception loss measurements; ii) main uncertainties depend on I_r and canopy size that can be measured and field validated; iii) although this was not done in this study, the dependence of I_r on per-species canopy size and environmental conditions can be investigated, adding additional credibility to the proposed method; and iv) images that are used for spatial upscaling, can be continuously improved with respect to accurate identification of objects' (trees') attributes (species type and canopy area or even canopy volume) by adding more spectral bands for species classification, stereoscopy and by improving spatial resolution of the images (e.g., Ferreira et al., 2016; Leckie et al., 2016; Pham et al., 2016). As such, the characteristics of the proposed method in this study, makes it particularly suitable for water-limited savannah type of environments, like for example the *dehesa* oak woodland in Spain, where trees are isolated, so their species classification and crown area estimates can be very accurately and efficiently automatized applying remote sensing techniques at multispectral, high resolution images.

Considering that tree interception loss can represent significant and important component of water balance, particularly in water limited environments, and that in most of water resources studies, the interception loss is lumped by its arbitrary assumptions (e.g., Goderniaux et al., 2009; Hassan, 2008; Hassan et al., 2014; Li et al., 2008; Liu et al., 2016; Massuel et al., 2013; Surfleet et al., 2012; Tian et al., 2015; Touhami et al., 2015), the proposed method offers valuable alternative to improve accuracy of tree interception loss estimates at large-scales such as catchments, where individual interception measurements of all trees are not feasible. As water resources studies are nowadays carried out by numerical distributed hydrological models, the proposed method is also suitable for its automated integration as input in such models.

5. Conclusions

The tree interception loss was measured in the sparsely vegetated Sardon catchment (~80 km^2) on two Mediterranean oak species occurring in that catchment, *Quercus ilex* (*Q.i.*) and *Quercus pyrenaica* (*Q.p.*) for two years. The measured tree interception loss was upscaled from the tree-scale into the plot- and catchment-scales, using remote sensing canopy area estimates; the method is presented applying measurement-related, simplifying assumption that the reference tree interception loss (flux), is dependent on species type but independent on tree size. The key findings are summarized below:

1. The single tree interception loss of evergreen *Q.i.* oak was 170 and 307 mm·y^{-1}, i.e., 50.7 and 45.7% of annual rainfall of 2012 (335 mm) and 2013 (672 mm), respectively. The relative interception loss was larger than reported in other studies, most likely because of low rainfall intensities, frequent occurrence of small rainfall events and low tree density which enhanced aerodynamic conductance.
2. The single tree interception loss of deciduous *Q.p.* oak was 53 and 66 mm·y^{-1}, i.e., 15.8% and 9.8% of annual rainfall of 2012 and 2013 respectively, so was in agreement with other studies. That interception loss was much lower than that of *Q.i.*, mainly because of 5-months leafless period when interception loss was negligible.
3. The revised Gash analytical model was able to reproduce well the measured cumulative interception loss for two trees, provided that *Tf*-based values for average wet-canopy evaporation rates were used.
4. The upscaling of tree interception loss depends mainly on field-defined, reference interception loss and species-specific canopy coverage that in small areas can be estimated directly in the field but in large areas by remote sensing identification of individual canopies on multi-spectral high resolution images.
5. The remote sensing upscaling of annual tree interception losses at two 1-ha homogeneous plots of *Q.i.* and *Q.p.*, both with ~20% canopy cover, in 2012 resulted in tree interception losses of 34 mm (10.1% of rainfall) for *Q.i.* and 10.6 mm (3.2% of rainfall) for *Q.p.* plot; and in 2013, 61 mm (9.1% of rainfall) for *Q.i.* and 13.2 mm (2.0% of rainfall) for *Q.p.* plot; the results were relatively low compared to similar plot estimates in other studies.
6. The remote sensing upscaling of annual tree interception losses in the Sardon catchment (~80 km^2) indicated catchment interception losses of 5.2 mm (1.6% of rainfall) in 2012 and 7.9 mm (1.2% of rainfall) in 2013; such low values were mainly because of low tree density (13 stems per ha; 7% canopy cover) and large contribution (77% of canopy coverage) of deciduous *Q.p.*, for 5 months leafless.
7. The proposed method of remote sensing upscaling of tree interception loss measurements is particularly suitable for large areas such as catchments, with sparsely vegetated trees, where individual tree canopies can be identified on high resolution images. These are typically water limited areas where interception loss represents large contribution in water balances, therefore our method is expected to have high relevance and broad applicability in such areas. The method can be applied at any time interval such as day, week, month, year or multi-year period.

Acknowledgements

The research was jointly funded by a PhD scholarship of European Union's Erasmus Mundus External Cooperation Window (EMMA lot 12) and ITC Research Fund. We would like to thank Alain Francés, Enrico Balugani and Thomas Berends for helping in the field works and monitoring network. We also like to thank Leonardo Reyes-Acosta for providing tree canopy area map and surveyed tree biometric dataset. The manuscript benefitted from the consecutive comments and suggestions from the editor-in-chief, two associate editors, and three anonymous reviewers of the journal, whose efforts are greatly appreciated.

References

Alcalá, F.J., Custodio, E., 2014. Spatial average aquifer recharge through atmospheric chloride mass balance and its uncertainty in continental Spain. Hydrol. Process. 28 (2), 218–236. doi: 10.1002/hyp.9556.

Bruijnzeel, L.A., Sampurno, S.P., Wiersum, K.F., 1987. Rainfall interception by a young Acacia auriculiformis (a. cunn) plantation forest in West Java, Indonesia: application of Gash's analytical model. Hydrol. Process. 1 (4), 309–319. doi: 10.1002/hyp.3360010402.

Calabuig, E.L., Gago Camallo, M.L., Gómez Gutiérrez, J.M., 1978. Influence of holm oak (Quercus ilex rotundifolia) in the distribution of rainfall (Influencia de la encina (Quercus rotundifolia lam.) en la distribución del agua de lluvia). Yearbook of Spanish Centre for Soil and Applied Biology, Vol-IV. CSIC – Institute of Guidance and Technical Assistance West, pp. 143–159.

Campos, P. et al., 2013. Mediterranean Oak Woodland Working Landscapes: Dehesas of Spain and Ranchlands of California. Landscape Series, 16. Springer, Dordrecht, Heidelberg, New York, London, p. 508. doi: 10.1007/978-94-007-6707-2.

Carlyle-Moses, D.I., Gash, J.H.C., 2011. Rainfall interception loss by forest canopies. In: Levia, D.F., Carlyle-Moses, D., Tanaka, T. (Eds.), Forest Hydrology and Biogeochemistry. Ecological Studies, Springer, Netherlands, pp. 407–423. doi: 10.1007/978-94-007-1363-5_20.

Cui, Y., Jia, L., 2014. A modified gash model for estimating rainfall interception loss of forest using remote sensing observations at regional scale. Water 6 (4), 993–1012.
David, J.S., Valente, F., Gash, J.H.C., 2005. Evaporation of intercepted rainfall. In: Anderson, M.G. (Ed.), Encyclopedia of Hydrological Sciences. John Wiley & Sons Ltd., Chichester UK, pp. 627–634.
David, T.S. et al., 2006. Rainfall interception by an isolated evergreen oak tree in a Mediterranean savannah. Hydrol. Process. 20 (13), 2713–2726.
Dykes, A.P., 1997. Rainfall interception from a lowland tropical rainforest in Brunei. J. Hydrol. 200 (1–4), 260–279. doi: 10.1016/S0022-1694(97)00023-1.
Fan, J., Oestergaard, K.T., Guyot, A., Lockington, D.A., 2014. Measuring and modeling rainfall interception losses by a native Banksia woodland and an exotic pine plantation in subtropical coastal Australia. J. Hydrol. 515, 156–165. doi: 10.1016/j.jhydrol.2014.04.066.
Ferreira, M.P., Zortea, M., Zanotta, D.C., Shimabukuro, Y.E., de Souza Filho, C.R., 2016. Mapping tree species in tropical seasonal semi-deciduous forests with hyperspectral and multispectral data. Remote Sens. Environ. 179, 66–78. doi: 10.1016/j.rse.2016.03.021.
Gärdenäs, A.I., Jansson, P.-E., 1995. Simulated water balance of Scots pine stands in Sweden for different climate change scenarios. J. Hydrol. 166 (1–2), 107–125. doi: 10.1016/0022-1694(94)02594-2.
Gash, J.H.C., 1979. Analytical model of rainfall interception by forests. Q. J. R. Meteorol. Soc. 105 (1979–4), 43–55.
Gash, J.H.C., Lloyd, C.R., Lachaud, G., 1995. Estimating sparse forest rainfall interception with an analytical model. J. Hydrol. 170 (1–4), 79–86.
Gash, J.H.C., Morton, A.J., 1978. An application of the Rutter model to the estimation of the interception loss from Thetford Forest. J. Hydrol. 38 (1–2), 49–58. doi: 10.1016/0022-1694(78)90131-2.
Ghimire, C.P., Bruijnzeel, L.A., Lubczynski, M.W., Bonell, M., 2012. Rainfall interception by natural and planted forests in the Middle Mountains of Central Nepal. J. Hydrol. 475, 270–280. doi: 10.1016/j.jhydrol.2012.09.051.
Ghimire, C.P., Bruijnzeel, L.A., Lubczynski, M.W., Bonell, M., 2014. Negative trade-off between changes in vegetation water use and infiltration recovery after reforesting degraded pasture land in the Nepalese Lesser Himalaya. Hydrol. Earth Syst. Sci. Discuss. 11 (3), 3437–3479. doi: 10.5194/hessd-11-3437-2014.
Ghimire, C.P. et al., 2017. Measurement and modeling of rainfall interception by two differently aged secondary forests in upland eastern Madagascar. J. Hydrol. 545, 212–225. doi: 10.1016/j.jhydrol.2016.10.032.
Goderniaux, P. et al., 2009. Large scale surface–subsurface hydrological model to assess climate change impacts on groundwater reserves. J. Hydrol. 373 (1–2), 122–138. doi: 10.1016/j.jhydrol.2009.04.017.
Gómez, J.A., Giráldez, J.V., Fereres, E., 2001. Rainfall interception by olive trees in relation to leaf area. Agric. Water Manage. 49 (1), 65–76. doi: 10.1016/S0378-3774(00)00116-5.
Hassan, S.M.T., 2008. Assessment of groundwater evaporation through groundwater model with spatio – temporally variable fluxes: case study of Pisoes catchment, Portugal (MSc thesis). ITC, Enschede, p. 97. Retrieved on April 30, 2017 from http://www.itc.nl/library/papers_2008/msc/wrem/tanvir.pdf.
Hassan, S.M.T., Lubczynski, M.W., Niswonger, R.G., Su, Z., 2014. Surface–groundwater interactions in hard rocks in Sardon Catchment of western Spain: an integrated modeling approach. J. Hydrol. 517, 390–410. doi: 10.1016/j.jhydrol.2014.05.026.
Henson, W.R., Medina, R.L., Mayers, C.J., Niswonger, R.G., Regan, R.S., 2013. CRT – Cascade Routing Tool to define and visualize flow paths for grid-based watershed models, U.S. Geological Survey Techniques and Methods 6-D2, 28 p.
Herwitz, S.R., 1987. Raindrop impact and water flow on the vegetative surfaces of trees and the effects on stemflow and throughfall generation. Earth Surf. Proc. Land. 12 (4), 425–432. doi: 10.1002/esp.3290120408.
Holwerda, F., Bruijnzeel, L.A., Scatena, F.N., Vugts, H.F., Meesters, A.G.C.A., 2012. Wet canopy evaporation from a Puerto Rican lower montane rain forest: the importance of realistically estimated aerodynamic conductance. J. Hydrol. 414–415, 1–15. doi: 10.1016/j.jhydrol.2011.07.033.
Hörmann, G. et al., 1996. Calculation and simulation of wind controlled canopy interception of a beech forest in Northern Germany. Agric. For. Meteorol. 79 (3), 131–148. doi: 10.1016/0168-1923(95)02275-9.
Jackson, I.J., 1975. Relationships between rainfall parameters and interception by tropical forest. J. Hydrol. 24 (3–4), 215–238. doi: 10.1016/0022-1694(75)90082-7.
King, B.P., Harrison, S.J., 1998. Throughfall patterns under an isolated oak tree. Weather 53 (4), 111–121. doi: 10.1002/j.1477-8696.1998.tb03973.x.
Le Maitre, D.C., Scott, D.F., Colvin, C., 1999. A review of information on interactions between vegetation and groundwater. Water SA 25 (2), 137–152.
Leckie, D.G., Walsworth, N., Gougeon, F.A., 2016. Identifying tree crown delineation shapes and need for remediation on high resolution imagery using an evidence based approach. ISPRS J. Photogrammetry Remote Sens. 114, 206–227. doi: 10.1016/j.isprsjprs.2016.02.005.
Levia, D.F., Frost, E.E., 2003. A review and evaluation of stemflow literature in the hydrologic and biogeochemical cycles of forested and agricultural ecosystems. J. Hydrol. 274 (1–4), 1–29. doi: 10.1016/S0022-1694(02)00399-2.
Levia, D.F., Frost, E.E., 2006. Variability of throughfall volume and solute inputs in wooded ecosystems. Prog. Phys. Geogr. 30 (5), 605–632. doi: 10.1177/0309133306071145.
Li, Q. et al., 2008. Simulating the multi-seasonal response of a large-scale watershed with a 3D physically-based hydrologic model. J. Hydrol. 357 (3–4), 317–336. doi: 10.1016/j.jhydrol.2008.05.024.
Limousin, J.-M., Rambal, S., Ourcival, J.-M., Joffre, R., 2008. Modelling rainfall interception in a mediterranean Quercus ilex ecosystem: lesson from a throughfall exclusion experiment. J. Hydrol. 357 (1–2), 57–66. doi: 10.1016/j.jhydrol.2008.05.001.
Liu, Z., Chen, H., Huo, Z., Wang, F., Shock, C.C., 2016. Analysis of the contribution of groundwater to evapotranspiration in an arid irrigation district with shallow water table. Agric. Water Manage. 171, 131–141. doi: 10.1016/j.agwat.2016.04.002.
Llorens, P., Domingo, F., 2007. Rainfall partitioning by vegetation under Mediterranean conditions. A review of studies in Europe. J. Hydrol. 335 (1–2), 37–54. doi: 10.1016/j.jhydrol.2006.10.032.
Llorens, P., Latron, J., Álvarez-Cobelas, M., Martínez-Vilalta, J., Moreno, G., 2011. Hydrology and biogeochemistry of mediterranean forests. In: Levia, D.F., Carlyle-Moses, D., Tanaka, T. (Eds.), Forest Hydrology and Biogeochemistry. Ecological Studies, Springer, Netherlands, pp. 301–319. doi: 10.1007/978-94-007-1363-5_14.
Llorens, P., Poch, R., Latron, J., Gallart, F., 1997. Rainfall interception by a Pinus sylvestris forest patch overgrown in a Mediterranean mountainous abandoned area I. Monitoring design and results down to the event scale. J. Hydrol. 199 (3–4), 331–345. doi: 10.1016/S0022-1694(96)03334-3.
Lloyd, C.R., Gash, J.H.C., Shuttleworth, W.J., de O. Marques F, A., 1988. The measurement and modelling of rainfall interception by Amazonian rain forest. Agric. For. Meteorol. 43 (3–4), 277–294. doi: 10.1016/0168-1923(88)90055-X.
Lubczynski, M.W., Gurwin, J., 2005. Integration of various data sources for transient groundwater modeling with spatio-temporally variable fluxes–Sardon study case, Spain. J. Hydrol. 306 (1–4), 71–96.
Lubczynski, M.W., 2009. The hydrogeological role of trees in water-limited environments. Hydrogeol. J. 17 (1), 247–259. doi: 10.1007/s10040-008-0357-3.
Markstrom, S.L., Niswonger, R.G., Regan, R.S., Prudic, D.E., Barlow, P.M., 2008. GSFLOW-Coupled Ground-water and Surface-water FLOW model based on the integration of the Precipitation-Runoff Modeling System (PRMS) and the Modular Ground-Water Flow Model (MODFLOW-2005), Techniques and Methods 6-D1. U.S. Geological Survey.
Massuel, S., George, B.A., Venot, J.P., Bharati, L., Acharya, S., 2013. Improving assessment of groundwater-resource sustainability with deterministic modelling: a case study of the semi-arid Musi sub-basin, South India. Hydrogeol. J. 21 (7), 1567–1580. doi: 10.1007/s10040-013-1030-z.
Mateos, B., Schnabel, S., 2001. Rainfall interception by Holm Oaks in Mediterranean open woodland. J. Geogr. Res. (Cuadernos de Investigación Geográfica) 27, 27–38.
MIMAM, 2000. White book of water in Spain. Ministry of the Environment, State Secretary of Waters and Coast. General Directorate of Hydraulic Works and Water Quality, Madrid, p. 637 [in Spanish]. (http://hercules.cedex.es/Informes/Planificacion/2000-Libro_Blanco_del_Agua_en_Espana/).
Miralles, D.G., Gash, J.H., Holmes, T.R.H., de Jeu, R.A.M., Dolman, A.J., 2010. Global canopy interception from satellite observations. J. Geophys. Res.: Atmos. 115 (D16), D16122. doi: 10.1029/2009JD013530.
Monteith, J.L., 1965. Evaporation and environment. Symposia Soc. Exp. Biol. 19, 205–234.
Morán, C.T., Fernández, J.M., Santana, V.H., Crespo, A.C., 2008. Throughfall and interception losses in a Forest Oak Melojo Central System (Trascolacion y perdidas por interceptacion en un Bosque de Roble Melojo del Sistema Central). J. Geog. Res. (Cuadernos de Investigacion Geografica) 34, 7–22.
Moreno, G., Gallardo, J.F., Bussotti, F., 2001. Canopy modification of atmospheric deposition in oligotrophic Quercus pyrenaica forests of an unpolluted region (central-western Spain). For. Ecol. Manage. 149 (1–3), 47–60. doi: 10.1016/S0378-1127(00)00544-2.
Murakami, S., 2006. A proposal for a new forest canopy interception mechanism: splash droplet evaporation. J. Hydrol. 319 (1–4), 72–82. doi: 10.1016/j.jhydrol.2005.07.002.
Murakami, S., 2009. Abrupt changes in annual stemflow with growth in a young stand of Japanese cypress. Hydrol. Res. Lett. 3, 32–35. doi: 10.3178/HRL.3.32.
Mużyło, A., Llorens, P., Domingo, F., 2012. Rainfall partitioning in a deciduous forest plot in leafed and leafless periods. Ecohydrology 5 (6), 759–767. doi: 10.1002/eco.266.
Nieschulze, J., Erasmi, S., Dietz, J., Hölscher, D., 2009. Satellite-based prediction of rainfall interception by tropical forest stands of a human-dominated landscape in Central Sulawesi, Indonesia. J. Hydrol. 364 (3–4), 227–235. doi: 10.1016/j.jhydrol.2008.10.024.
Peng, H.H. et al., 2009. Modeling canopy interception of Picea Crassifolia forest in Qilian Mountains using QuickBird satellite data. 2009 IEEE International Geoscience and Remote Sensing Symposium, vol. 1–5. IEEE, New York, pp. 2750–2753.
Pereira, F.L. et al., 2009a. Modelling interception loss from evergreen oak Mediterranean savannas: application of a tree-based modelling approach. Agric. For. Meteorol. 149 (3–4), 680–688. doi: 10.1016/j.agrformet.2008.10.014.
Pereira, F.L., Gash, J.H.C., David, J.S., Valente, F., 2009b. Evaporation of intercepted rainfall from isolated evergreen oak trees: do the crowns behave as wet bulbs? Agric. For. Meteorol. 149 (3–4), 667–679.
Pereira, F.L. et al., 2016. Rainfall interception modelling: is the wet bulb approach adequate to estimate mean evaporation rate from wet/saturated canopies in all forest types? J. Hydrol. 534, 606–615. doi: 10.1016/j.jhydrol.2016.01.035.
Pham, L.T.H., Brabyn, L., Ashraf, S., 2016. Combining QuickBird, LiDAR, and GIS topography indices to identify a single native tree species in a complex landscape using an object-based classification approach. Int. J. Appl. Earth Obs. Geoinf. 50, 187–197. doi: 10.1016/j.jag.2016.03.015.

Qi, J. et al., 2000. Leaf area index estimates using remotely sensed data and BRDF models in a semiarid region. Remote Sens. Environ. 73 (1), 18–30. doi: 10.1016/S0034-4257(99)00113-3.

Reyes-Acosta, J.L., Lubczynski, M.W., 2013. Mapping dry-season tree transpiration of an oak woodland at the catchment scale, using object-attributes derived from satellite imagery and sap flow measurements. Agric. For. Meteorol. 174–175, 184–201. doi: 10.1016/j.agrformet.2013.02.012.

Schellekens, J., Scatena, F.N., Bruijnzeel, L.A., Wickel, A.J., 1999. Modelling rainfall interception by a lowland tropical rain forest in northeastern Puerto Rico. J. Hydrol. 225 (3–4), 168–184. doi: 10.1016/S0022-1694(99)00157-2.

Surfleet, C.G., Tullos, D., Chang, H., Jung, I.-W., 2012. Selection of hydrologic modeling approaches for climate change assessment: a comparison of model scale and structures. J. Hydrol. 464–465, 233–248. doi: 10.1016/j.jhydrol.2012.07.012.

Tárrega, R., Calvo, L., Taboada, Á., García-Tejero, S., Marcos, E., 2009. Abandonment and management in Spanish dehesa systems: effects on soil features and plant species richness and composition. For. Ecol. Manage. 257 (2), 731–738. doi: 10.1016/j.foreco.2008.10.004.

Teklehaimanot, Z., Jarvis, P.G., Ledger, D.C., 1991. Rainfall interception and boundary layer conductance in relation to tree spacing. J. Hydrol. 123 (3–4), 261–278. doi: 10.1016/0022-1694(91)90094-X.

Terradas, J., 1999. Holmoak and holm oak forests: an introduction. In: Roda, F., Retana, J., Gracia, C.A., Bellot, J. (Eds.), Ecology of Mediterranean Evergreen Oak Forests. Springer, Berlin, pp. 3–14.

Thom, A.S., 1975. Momentum, mass and heat exchange of plant communities. In: Monteith, J.L. (Ed.), Vegetation and the Atmosphere, Principles, vol 1. Academic Press, London, pp. 57–109.

Tian, Y. et al., 2015. Exploring scale-dependent ecohydrological responses in a large endorheic river basin through integrated surface water-groundwater modeling. Water Resour. Res. 51 (6), 4065–4085. http://dx.doi.org/10.1002/2015WR016881.

Tiktak, A., Bouten, W., 1994. Soil water dynamics and long-term water balances of a Douglas fir stand in the Netherlands. J. Hydrol. 156 (1–4), 265–283. doi: 10.1016/0022-1694(94)90081-7.

Touhami, I. et al., 2015. Assessment of climate change impacts on soil water balance and aquifer recharge in a semiarid region in south east Spain. J. Hydrol. 527, 619–629. doi: 10.1016/j.jhydrol.2015.05.012.

Valente, F., David, J.S., Gash, J.H.C., 1997. Modelling interception loss for two sparse eucalypt and pine forests in central Portugal using reformulated Rutter and Gash analytical models. J. Hydrol. 190, 141–162.

van Dijk, A., Bruijnzeel, L.A., 2001. Modelling rainfall interception by vegetation of variable density using an adapted analytical model. Part 1. Model description. J. Hydrol. 247 (3–4), 230–238.

van Dijk, A.I.J.M. et al., 2015. Rainfall interception and the coupled surface water and energy balance. Agric. For. Meteorol. 214–215, 402–415. doi: 10.1016/j.agrformet.2015.09.006.

Wallace, J., McJannet, D., 2008. Modelling interception in coastal and montane rainforests in northern Queensland, Australia. J. Hydrol. 348 (3–4), 480–495. doi: 10.1016/j.jhydrol.2007.10.019.

Xiao, Q., McPherson, E.G., Ustin, S.L., Grismer, M.E., 2000a. A new approach to modeling tree rainfall interception. J. Geophys. Res. 105 (D23), 29173–29188.

Xiao, Q., McPherson, E.G., Ustin, S.L., Grismer, M.E., Simpson, J.R., 2000b. Winter rainfall interception by two mature open-grown trees in Davis, California. Hydrol. Process. 14 (4), 763–784. doi: 10.1002/(sici)1099-1085(200003)14:4<763::aid-hyp971>3.0.co;2-7.

Yang, D.Q. et al., 1999. Wind-induced precipitation undercatch of the Hellmann gauges. Nord. Hydrol. 30 (1), 57–80.